

https://dspace.org/

Densification, microstructure and properties of liquidphase sintered silicon carbide materials

Can, Antionette

2006-02-06
http://hdl.handle.net/10539/172

Downloaded from a DSpace repository. https://dspace.org/

2. LITERATURE REVIEW

2.1 History / background of Silicon Carbide

The formation of silicon carbide was first reported by Berzelius in 1824[1], and was observed in laboratory experiments by Despretz[25], Schuetzenberger[26] and Moissan[27], between 1824 and 1881. Moissan found natural SiC in a meteorite in 1905[27], which is the origin of the mineral name of silicon carbide, which is "Moissanite". As already stated in the Chapter 1, it was only after the invention of the electric smelting furnace by Cowles[2] in 1885, followed by the development of the Acheson process[3] , that silicon carbide's technical importance as a hard material was realised.

The development of the Acheson process made the large scale production of silicon carbide possible by 1891. The discovery that silicon carbide could be produced by this process was "accidental". Acheson had originally wanted to produce artificial diamond by recrystallising graphite in an aluminium silicate melt. He believed that he had formed a compound of carbon and corundum (aluminium oxide), and hence called the resultant material "carborundum" (which is the common name for silicon carbide in the abrasives industry today.) Acheson did not succeed in making artificial diamond, but instead formed a more versatile material, silicon carbide[4].

Today, silicon carbide is produced on a large scale by the Acheson/ESK process. This process involves the reaction between high purity quartz (99.5% SiO_2) and petroleum coke in electrically heated resistance furnaces. The reaction here is:

$$SiO_2 + 3C = SiC + 2CO. \qquad (2.1)$$

The process takes place between 1600^{o}C and 2500^{o}C, in furnaces up to 25 metres long, 4 metres wide and 4 metres high. A schematic

representation of an Acheson/ESK furnace is shown in Figure 2.1. The furnaces can consume up to 5000kVA, and the process can run for up to about 130 hours.

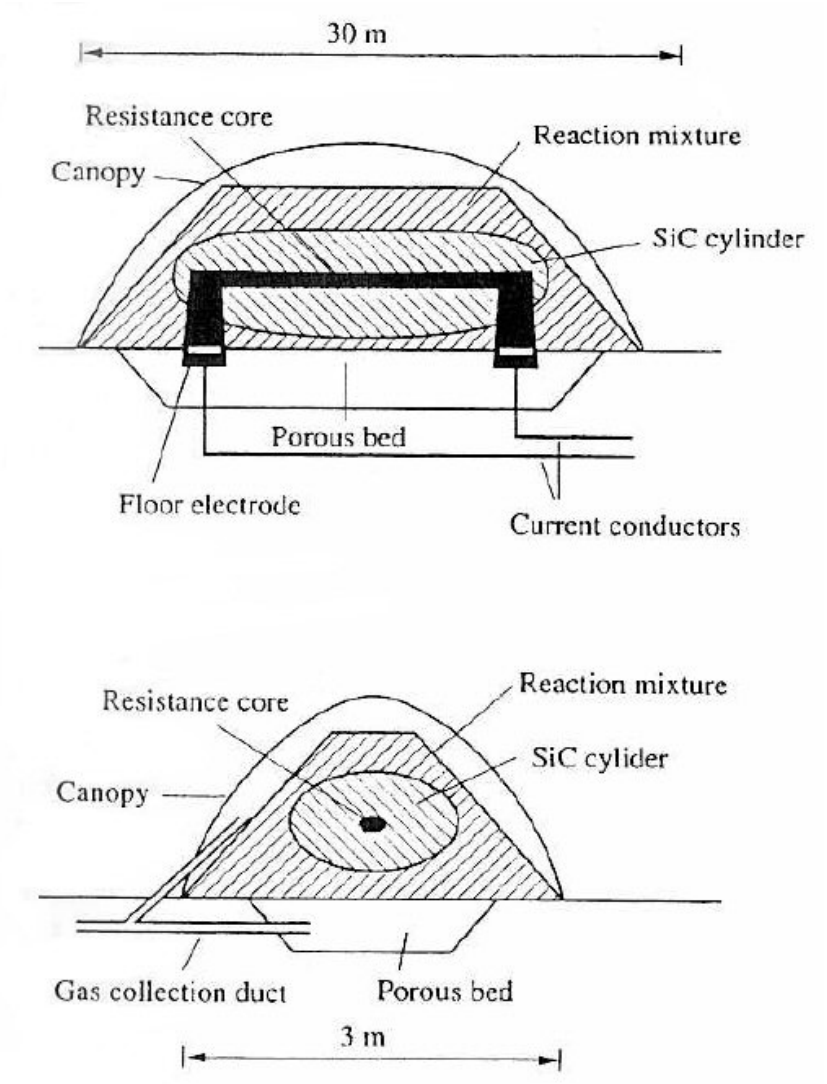


Figure 2.1 The Acheson furnace in a) longitudinal and b) cross-section[4]

This process produces silicon carbide crystals, which are then milled and purified to obtain a commercial grade silicon carbide powder, which can be sintered to produce different silicon carbide materials.

There are many other methods which have been developed to produce silicon carbide. Carbothermal reduction of silica has been used to produce pure ultra-fine β-SiC for the semiconductor and pigment industry[28,29]. Later the process was modified to produce β-SiC powder[30,31]. α-SiC platelets, are commercially produced using silicon, carbon and micron-sized β-SiC powders at temperatures between 1900- 2100°C. Aluminium and boron dopants are used to produce platelet-shaped crystals. Aluminium enhances growth in the [0001] direction and decelerates growth perpendicular to the [0001] direction. Boron, on the other hand, enhances growth perpendicular to the [0001] direction[32]. For example, SiC platelets produced by the company "Millenium Materials", contain 0.04 – 0.45 mass-% aluminium, 0.4 -0.8 mass-% boron and nickel (each), and 0.3 -3.6 mass-% silicon[33]. High resolution AES revealed that most impurities were present on the outermost surfaces of the platelets[33].

In the 20th century, methods have also been developed to synthesise SiC whiskers[34] and SiC fibres[35].

Self-bonded silicon carbide materials in molded form and with a high silicon carbide content, have only been made available since the late 1960's. It was only in the early 1970's that the first "dense" (less than 2 % porosity) silicon carbide materials were made. In 1973 Prochazka[7] sintered β-SiC to high densities, using boron and carbon additives, at about 2100°C. This was the advent of solid-state sintered silicon carbide (SSiC). Following Prochazka, Coppola *et al.*[36] found that α-SiC powders could also be densified under similar conditions. In 1981 the idea of alloying Al_2OC and/ or AlN with SiC[37] to form solid solutions, was first introduced, since these carbides and nitrides and SiC-2H polytype are isostructural.

Liquid phase sintering, with oxide additives, as a means of densifying silicon carbide, was initiated in 1982 by Omori et al[8]. They showed that β-

silicon carbide could be densified by pressureless sintering at 2100^{o}C, using yttrium and aluminium hydroxide precursors, which reacted and formed oxides, and facilitated densification via liquid-phase sintering. The successful liquid phase sintering of silicon nitride (Si_3N_4) with the Y_2O_3-Al_2O_3 sintering additive system also lead to many groups successfully densifying α-SiC and β-SiC with these additives, since the late 1980's[10, 38, 39, 40, 41, 42].

Lee *et al.*[43] successfully liquid phase sintered SiC using AlN together with yttria and /or alumina. This success was followed by the work of Chia *et al.*[44] and Nader[45] which showed that silicon carbide sintered with the Y_2O_3-AlN system has the advantage that decomposition reactions during sintering can be suppressed by application of a nitrogen overpressure.

Currently, the most commonly used sintering additives in liquid phase sintering of silicon carbide are the Y_2O_3-Al_2O_3 and Y_2O_3-AlN systems. The details of these systems and other methods of producing silicon carbide-based materials, will be discussed in further detail in sections 2.4, 2.5 and 2.6.

2.2 Crystal structure of silicon carbide

Silicon carbide crystals, as obtained by the Acheson process, are found in a number of modifications with either hexagonal, trigonal, or cubic symmetry. The silicon carbide structure consists of sp^3 hybridised atomic orbitals, forming tetrahedra with Si or C atom at the spatial centre, surrounded by four of the other atoms, crystallising in a diamond lattice like silicon[4]. The tetrahedra are arranged so that carbon atoms form closed packed parallel layers and Si is situated in the tetrahedron holes between the layers. These layer sequences can repeat themselves in cycles, for example, ABC, ABC (zinc blende-type structure) or AB, AB (wurtzite- type structure) with cubic or hexagonal close packing. According

to the close packing arrangement of the silicon and carbon atoms, silicon carbide is divided into α-SiC and β-SiC. α-SiC denotes the structures with hexagonal close-packing, and β-SiC denotes the structure with cubic close packing, which corresponds to the zinc-blende-type structure (with ABC, ABC repeating sequences).

Within the α–SiC group, there are a number of modifications with hexagonal or trigonal symmetry. These structures are all very similar, with nearly constant "a" axis and along the "c"-axis, changing as the repeat layer structure changes. These structures consist of identical layers perpendicular to the hexagonal c axes. The repeating units are carbon atoms surrounded by four silicon atoms in a tetrahedron. The stacking of these identical layers differ in terms of their repetition distance. This one-dimensional form of polymorphism was called polytypism by Baumhauer[46,47]. Many stacking sequences exist, making up the different polytypes of SiC, which all have similar properties and the same density (3.21 g/cm^3). About 180 different polytypes are known.

Ramsdell notation[48] is used to name the different polytypes of silicon carbide. This nomenclature is written with a number first, indicating the number of layers in the "repeating layer pack", followed by the crystal system C (cubic), H (hexagonal) or R (rhombohedral)[4]. The most commonly occurring polytypes are 3C, 2H, 4H, 6H and 15R, which are called short-period polytypes. The long-period polytypes are much less common and consist of blocks of short period polytypes "broken" by regularly occurring stacking faults[4]. The cubic form of SiC (3C) is referenced as β-SiC, as shown in Figure 2.2, all the hexagonal and rhombohedral polytypes are known as α-SiC (an example of which is shown in Figure 2.3).

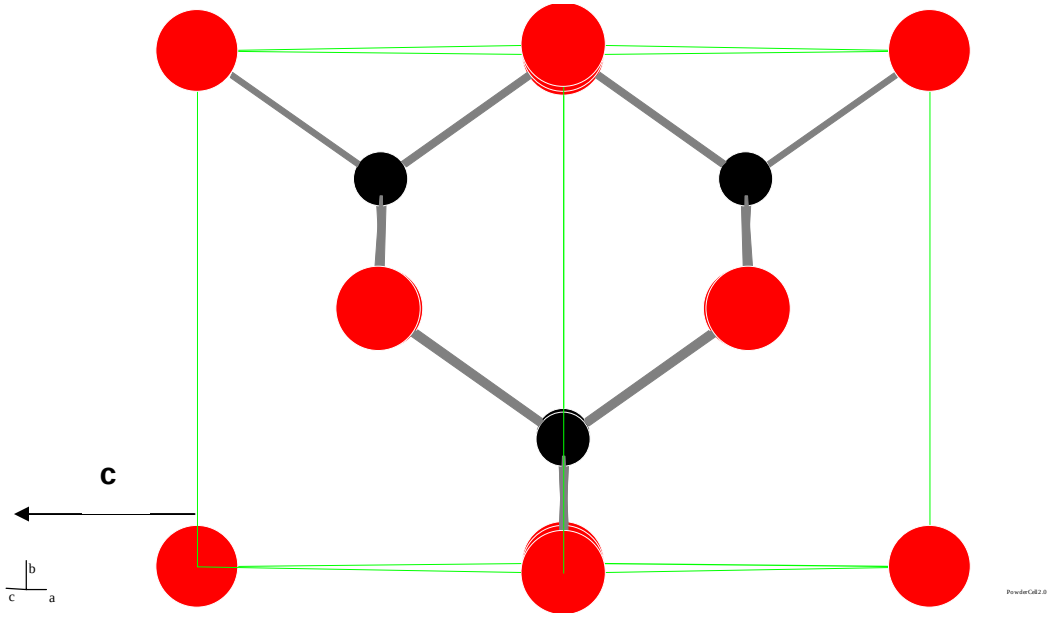


Figure 2.2 Projection of the crystal structure of 3C-SiC

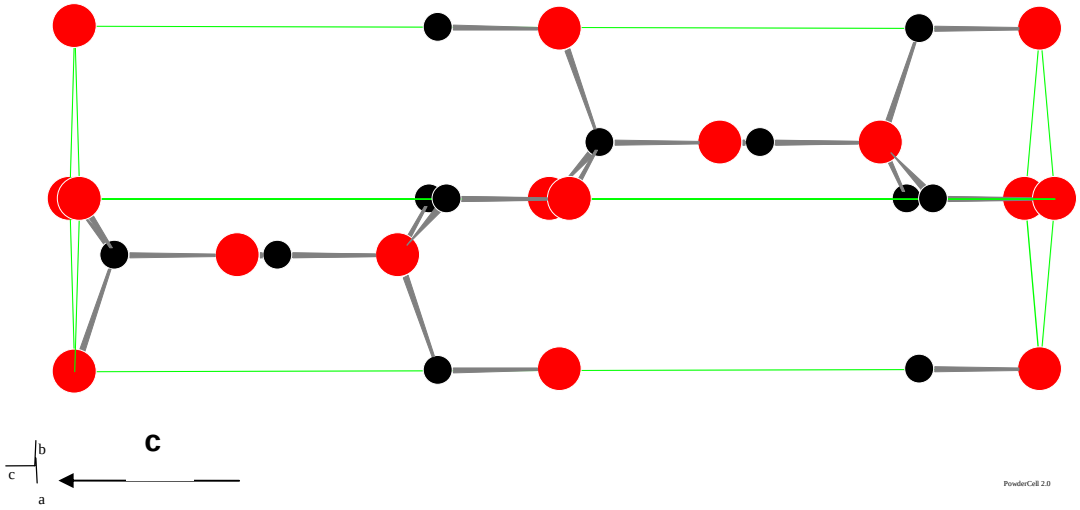


Figure 2.3 Projection of the crystal structure of 6H-SiC

β -SiC has been traditionally called the "low temperature modification" [4], a metastable phase at room temperature, which transforms to one or more of the polytypic forms of the α -SiC phase at elevated temperatures. It was said that above 2000°C β-SiC will not exist, unless there are some

stabilizing agents raising the transformation temperature[4]. However, work in a Philips research group in 1963[49] showed that the formation of β-SiC is not limited to low temperatures, and therefore should not be called the low-temperature modification of silicon carbide. This research also proved that cubic silicon carbide is unstable at all temperatures[49].

The formation mechanisms and thermodynamic stability of all the different polytypes are not clearly understood. It is believed that temperature, impurities, gas atmosphere and growth kinetic processes have an influence on the stability of the different polytypes. According to Inomata *et al.*[50] 2H-SiC is stable below 1400°C, 3C between 1400 and 1600°C, 4H between 1600 and 2100°C, 6H above 2100°C and 15R above 2200°C. Additions of up to 0.4 mass-% Al is believed to stabilize the 4H polytype, by substitution of Al for Si in the SiC lattice[51-54]. According to Lundquist[51] α-SiC crystallizes as mainly 6H polytype. If there is a small amount of Al (less than 0.1 mass%), 15R is stabilized, whereas more than 0.1 mass% Al is supposed to stabilize the 4H polytype. These relationships are illustrated in Figure 2.4 below.

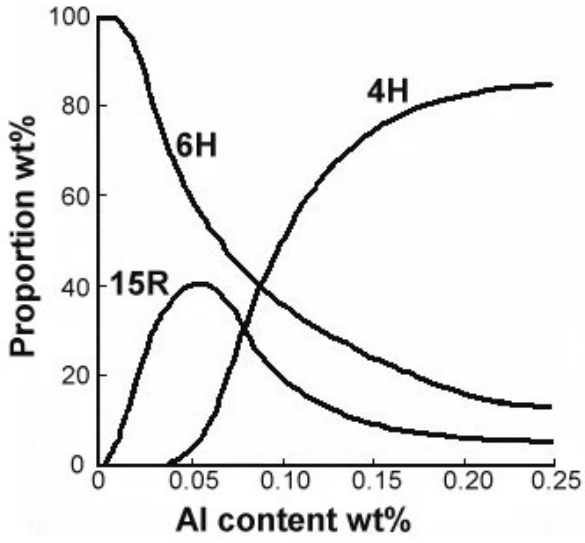


Figure 2.4 Relationship between SiC polytype stability and Al content[4]

However, Lundquist's relationships between statistical distribution of silicon carbide polytypes and aluminium content, in Figure 2.4, did not include the effect of temperature. Knippenberg[49] (Philips research) found that there was no definite relationship between impurity content and structure, in crystals with different amounts of aluminium grown at a fixed temperature. They did however find that acceptor impurities have a preference for and tend to stabilize hexagonal crystal structures, and donors tend to stabilize cubic structures[49].

Nitrogen-doping, when sintering in N_2 gas atmosphere, is also known to stabilize 3C and 2H [55,56]. Foster[57] produced silicon carbide polytypes by carbothermal reduction of silicon nitride in the presence of a liquid phase. Foster also found that gas/solid diffusion of nitrogen into 3C was low (less than 1 atom-%), whereas diffusion of nitrogen into 2H was high, up to 14 atom-% in the specimens that they prepared.

These SiC phase transformations (and their kinetics) have a great influence on the microstructural evolution of SiC-based ceramics and their related mechanical properties. Figure 2.5 shows an example of when purely α-SiC powders are sintered, and equiaxed microstructures of hexagonal shaped grains are obtained.

β-SiC starting powder, sintered with Y_2O_3-Al_2O_3 additives, and followed by a heat treatment, allows for *in-situ* toughening of silicon carbide. The β to α transformation, which takes place during the heat treatment, results in enhanced grain growth in the "c"-direction. This results in elongated α-SiC platelets in the microstructure, which toughen the materials[10]. An example of an *in-situ* toughened microstructure is given in Figure 2.6. The microstructure-to-properties relationships will be discussed in greater detail in section 2.6.4.

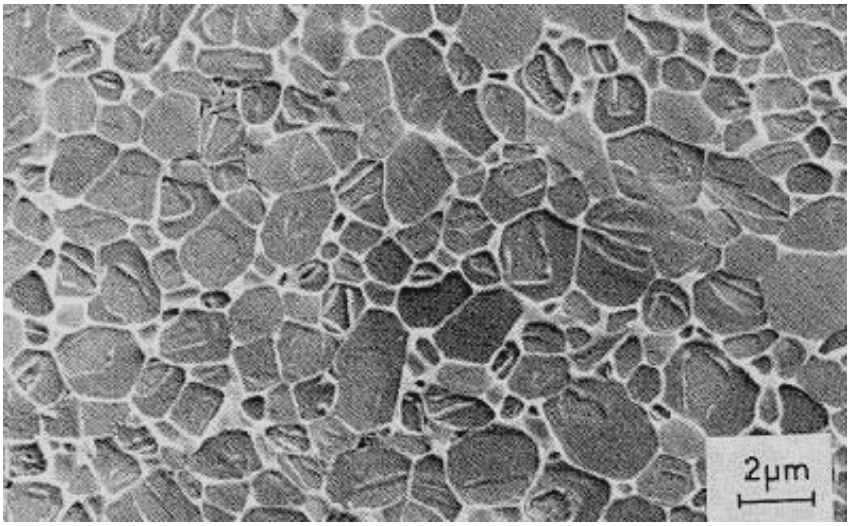


Figure 2.5 LPSSiC material microstructure showing equiaxed grains[4]

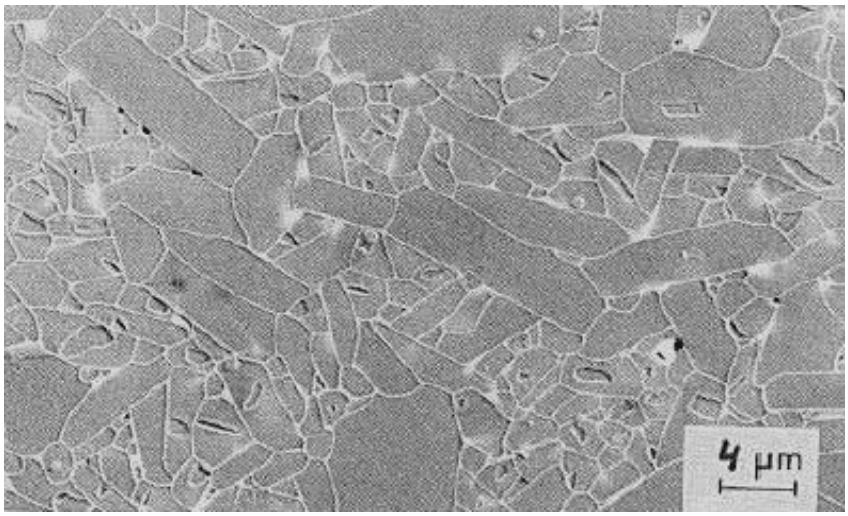


Figure 2.6 In-situ toughened microstructure of an LPSSiC material[4].

Usually the silicon carbide grains in a polycrystalline silicon carbide material are either predominantly β-SiC or α-SiC. However, within a single grain, a number of polytypes can exist, with stacking faults between them. High resolution lattice imaging techniques in transmission scanning electron microscopy can be used to analyse the distribution of the polytypes in single grains[58,59].

The free energies of all the different polytypes are so close that they often crystallize as a mixture of metastable phases. Since the crystal structures of the different silicon carbide polytypes are so similar, there is significant overlap between the Bragg reflections from the different polytypes. This makes the task of quantitative silicon carbide polytype determination difficult. Note that very fine grain size or high strain in the material would cause line broadening. Therefore, this would add to the difficulty of quantitative phase determination in any silicon carbide material. X-ray diffraction in conjunction with Rietveld refinement analysis, in principle, can be used for successful determination of SiC polytype content, limited success in this field of work has only been reported by two groups in the literature, namely Ortiz *et al.*[60 -64] and Hongchao *et al.*[65].

2.3 Properties of pure silicon carbide

Silicon carbide, is a high-temperature structural material, offering many advantages such as high melting temperatures, low density, high elastic modulus and strength, and good resistance to creep, oxidation and wear. These properties make SiC suitable for use in applications such as gas turbines, piston engines and heat exchangers, and where load-bearing components are required to operate at temperatures up to 1500^{o}C. The reason for SiC not realizing its full application potential, is its inherent lack of fracture toughness (typically 2-3 MPam$^{1/2}$ for monolithic SiC)[66].

The industrial importance of SiC is mainly due to its high hardness of 20-27GPa.

Silicon carbide does not have a congruent melting point. In a closed system of 1 bar pressure, SiC decomposes at 2830± 40^{o}C into graphite and molten Si. In an open system silicon carbide decomposes at about 2300^{o}C, into gaseous silicon and a residue of graphite[4].

Silicon carbide is a good semiconductor, with an energy band gap of close to 3 eV for the hexagonal structures[67] and 2.2 eV for the cubic structure[68]. Donor and acceptor impurities, can be found in small quantities in the silicon carbide structure, as a result of the silicon carbide synthesis process. These impurities can range from 0.04 mass-% to 0.8 mass-% of the silicon carbide[33].

Even in "high purity" commercial silicon carbide there are trace amounts of impurities, for example the "UF15SiC" powder from H.C. Starck. The data sheet of this powder shows that there can be up to 0.03 mass-% Al, 0.01 mass-% Ca, and 0.05 mass-% Fe[69]. These are low amounts of impurities, but their presence can have a significant influence on the band gap energies of the material sintered from this silicon carbide powder, as well as the electrical properties of this "pure" silicon carbide material in general. In addition to this, limited oxidation of silicon carbide in air results in a layer of silicon oxide (SiO_2) forming around the silicon carbide particles. This means that, depending on the particle size and surface area of the silicon carbide material, there is a certain mass-% SiO_2 present. For example, the fine-grained (d50=0.5µm) UF15 SiC powder can contain up to 1.5 mass-% oxygen[69]. In terms of mechanical properties, the powders can be considered to be "pure", however, when one is considering electrical properties, the definition of "pure" silicon carbide, is far more rigorous.

2.4 Overview of Different Silicon Carbide Materials and their Properties

Silicon carbide materials can be made by using additives to help bond the silicon carbide particles together, at elevated temperatures, without dimensional change, or with dimensional change by sintering, is the most common method of producing dense silicon carbide materials. Sintering is defined as a process of mass transport, at the atomic level, which bonds the particles together, resulting in elimination of porosity and shrinkage of

the body. This is combined with the growth of particles and forming of strong bonding between adjacent particles.

In this section, the most common silicon carbide materials will be introduced, which can be divided into two groups. The first group are the bonded silicon carbide materials, which are not dense. These include Ceramically–bonded Silicon Carbide (CSiC), Recrystallised Silicon Carbide (RSiC), Reaction-Bonded Silicon Carbide (RBSiC). The second group are the sintered, dense silicon carbide materials, which include Solid-state sintered Silicon Carbide (SSiC), Liquid-Phase Sintered Silicon Carbide (LPSSiC) and Silicon-infiltrated Silicon Carbide (SiSiC). Some properties of these silicon carbide materials are summarized in Table 2.1 below.

Table 2.1 Physical properties of different types of silicon carbide materials[4]

SiC material type	**ρ (g. cm^{-3})**	**Porosity (%)**	**Young Modulus (GPa)**	**Thermal conductivity at 600°C (WmK^{-1})**	**Flexural strength at RT (MPa)**	**Flexural strength at 1400°C (MPa)**
Ceramic bonded SiC [CSiC]	2.55	20	100	16	30	20
Re-crystallized SiC [RSiC]	2.60	20	250	28	100	100
Reaction bonded SiC [RBSiC]	2.60	20	250	25	250	250
Infiltrated SiC [SiSiC]	3.12	< 1	400	60	350	200
Solid-state sintered SiC [SSiC]	3.15	< 2	410	50	430	450
Liquid phase sintered SiC [LPSSiC]	3.21	< 1	420	50	730	400
Hot-pressed SiC [HPSiC]*	3.20	0	450	55	640	650
Hot-isostatic-pressed [HIPSiC]*	3.21	0	450	75	640	610

***** These methods of densifying silicon carbide will be discussed in the next section (2.5).

2.4.1 Ceramically bonded Silicon Carbide (CSiC)

In this type of material the silicon carbide grains are bonded together by oxide or nitride phases, for example, silicon nitride-bonded silicon carbide. The porosity of these materials can be up to 20 volume-%. To make CSiC materials coarse silicon carbide powders are mixed with clay or oxides like SiO_2 and/or Al_2O_3. These mixtures are formed into green bodies and fired at 1400^{o}C, which loosely bonds the silicon carbide particles together.

These porous materials are suitable for applications like refractory furnace bricks and abrasive discs. Silicon nitride- bonded silicon carbide can be made by firing silicon carbide in a nitrogen atmosphere (an example of this material's microstructure is given in Figure 2.7). In the presence of air this would yield silicon oxynitride-bonded SiC and if Al_2O_3 was added too, then this would result in SiAlON- bonded SiC[4].

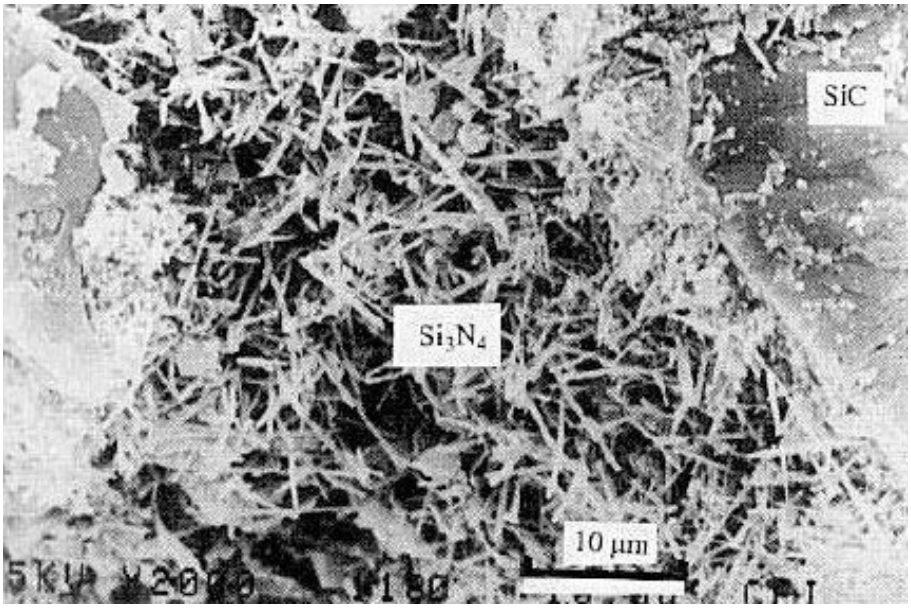


Figure 2.7 Silicon-nitride bonded silicon carbide material (CSiC)[4]

2.4.2 Recrystallised Silicon Carbide (RSiC)

Recrystallised silicon carbide materials are made from slip casted or press molded silicon carbide green bodies of bimodal grain size distribution. The high green density body is fired up to 2500°C in vacuum[70,71], which causes the evaporation and condensation[72,73] of silicon carbide. The result is a porous (approximately 20 volume-% porosity) self-bonded silicon carbide ceramic with the same density as the green density, which was about 2.6 g/cm^3. This pure silicon carbide material displays only a transgranular fracture mode, which results in low toughness. The microstructure of such a material is given in Figure 2.8 below.

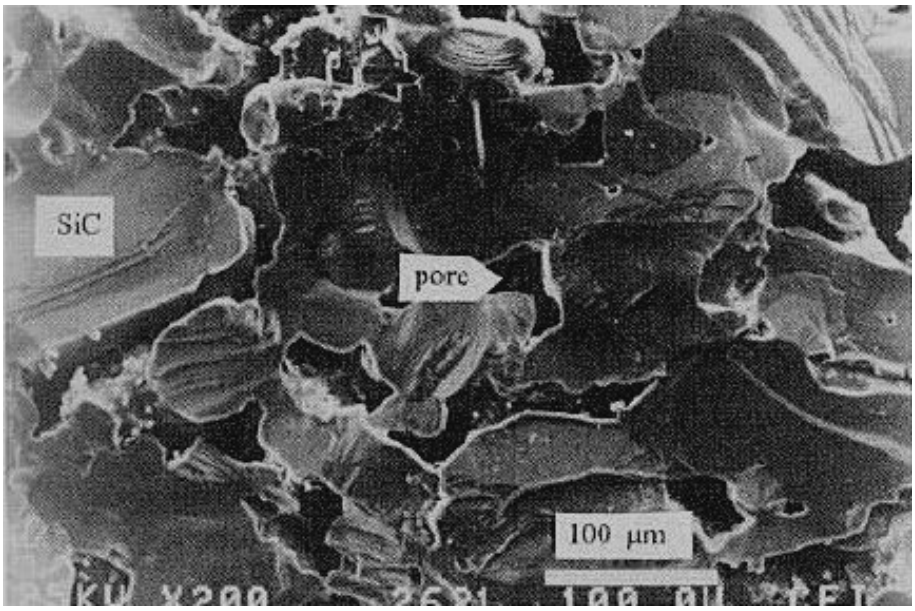


Figure 2.8 SEM micrograph of RSiC material[4]

2.4.3 Reaction-Bonded Silicon Carbide (RBSiC)

The synthesis of RBSC materials involves the forming of a green body mixture of SiC particles (5 – 10 μm), carbon, and a polymeric binder (for example polyurethane), by pressing, extrusion or injection moulding. In some cases silicon carbide and a carbon-forming resin is used. The binder/ resin is burned or pyrolysed to carbon. The porous preform is then

infiltrated with liquid Si at around 1410^{o}C (above the melting point of Si), resulting in the following reaction (2.2):

$$Si(l) + C (l) \rightarrow SiC (s). \quad (2.2)$$

The sintering occurs by the precipitation of the newly formed SiC product on the existing SiC grains, bonding them together. The microstructure of the RBSC generally consists of SiC grains coated by newly formed silicon carbide, with a network of residual silicon.

In reaction bonding sintering most commonly 90 vol.-% SiC is used with 10 vol.-% Si. The residual Si in the RBSC material degrades the mechanical strength of the material above 1200^{o}C, and for this reason alloying elements, such as 2 at.-% Mo is often added with the Si, to form refractory silicides (which are more chemically stable) like $MoSi_2$. RBSSiC have porosities up to 20 vol- %. The advantage of this method is little or no shrinkage, which allows for achieving of very close dimensional tolerances. With this advantage, reaction bonding is used to large scale production of silicon nitride (RBSN) and silicon carbide (RBSC) parts[74].

2.4.4 Silicon-infiltrated Silicon Carbide (SiSiC)

This is a type of reaction bonded silicon carbide material. The method used to make SiSiC is the same as described in section 2.4.3 above, except that excess silicon is infiltrated into the silicon carbide-resin structure, filling the pores. The result of the heat treatment is a dense silicon- infiltrated silicon carbide material, as shown in Figure 2.9.

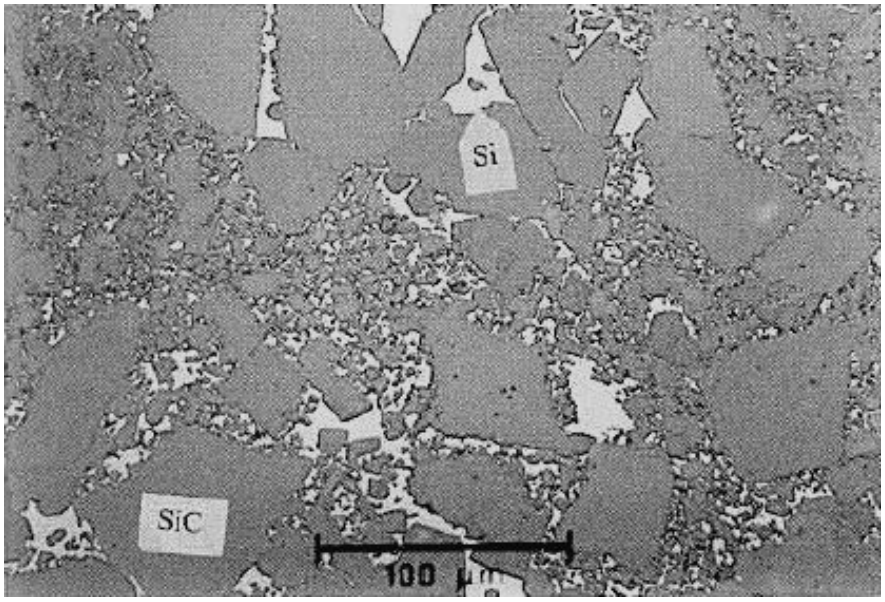


Figure 2.9 Microstructure of SiSiC material[4]

2.4.5 Sintered silicon carbide: Solid-state sintered Silicon Carbide (SSiC) vs Liquid-Phase Sintered Silicon Carbide (LPSSiC)

The sintering process occurs by mass transport at high temperature and sometimes a high pressure is also required as a driving force.

The driving force for solid- state sintering is the reduction of surface free energy of the particles, which is achieved either by atomic diffusion transporting matter from inside the grains to fill the pores (densification) or rearrangement of the matter between different parts of the pore surfaces (without reducing pore volume) coarsens the microstructure[75].

The first stage of solid state sintering is interparticle neck growth by diffusion, vapour transport, plastic flow or viscous flow. Most of the sintering takes place in the intermediate stage, in which the network of open porosity shrinks and pinches off leaving only ca. 10 % closed porosity. The final stage of sintering starts with the formation of only closed porosity, with a shrinkage of these closed pores until they disappear (if densification is full)[76].

Coarsening of the grains reduces the driving force for densification, hence sintering can be viewed as a competition between coarsening and densification.

The effects of temperature, grain size, applied pressure and gaseous atmosphere on the densification and coarsening processes are well understood. Increased temperature and reduced grain size increase the rates of densification and coarsening, whereas increase in applied pressure increases the rate of densification only. In recent years it has been realized that inhomogeneities in density, grain size and composition in the green body hinders the ability to fully densify that green body[(75)].

In solid-state sintering coarsening tends to dominate over densification, especially in highly covalent ceramics such as silicon nitride and silicon carbide. This makes it impossible to fully densify (to greater than 98% of its theoretical density) these covalent ceramics without any additives to aid the sintering. In solid-state sintering, the only transport mechanism is atomic diffusion in the solid state, and because of the fact that the bonding in silicon carbide is 80 % covalent, self-diffusivity is very low and pure silicon carbide could not be sintered to full density.

Solid state diffusion is defined by the definite path along which the diffusional mass transport takes place. Figure 2.10 shows the main mechanisms involved in sintering. Surface diffusion, lattice diffusion from the particle surfaces to the neck, and vapour transport in Figure 2.10[(77)] cause neck growth without densification (non-densifying mechanisms). Densification in polycrystalline ceramics occurs mainly by grain boundary diffusion and lattice diffusion from grain boundary to pore (mechanisms 4 and 5 in Figure 2.10)[(77)].

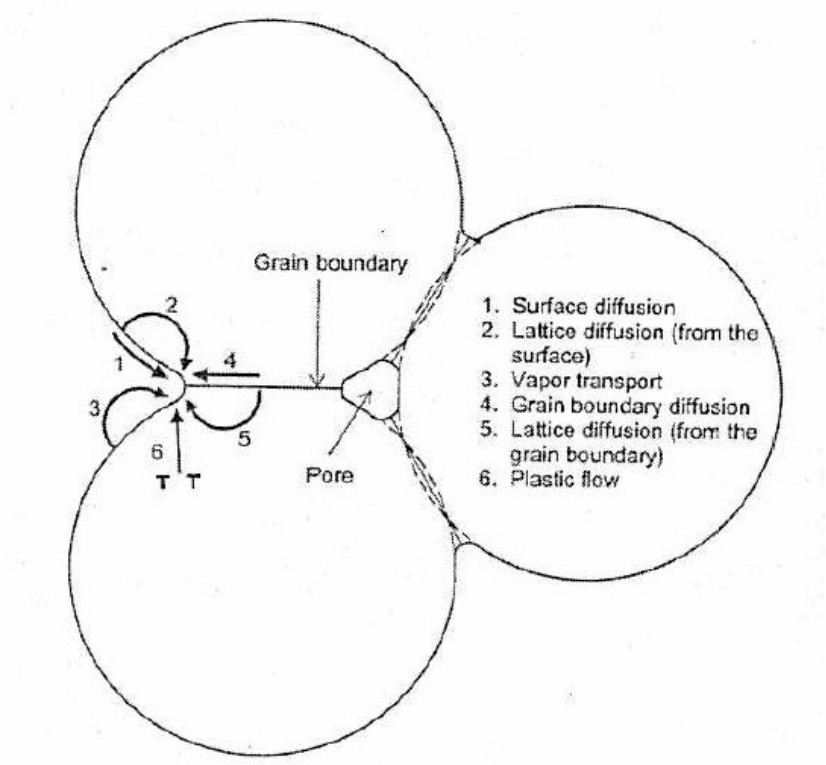


Figure 2.10 Difffusion paths for coarsening and densification[77]

Work by Prochazka led to first β-SiC[78] and later α-SiC[79] being pressureless-sintered with up to 2 % boron and carbon as sintering aids. A minimum of 0.3 mass-% boron was required for this, although more did not improve densification. Prochazka argued that this was because the solubility limit of boron in silicon carbide needed to be exceeded and according to Schaffer this limit is 0.2 mass-%[80]. Instead of boron, it was found that other boron compounds can also be used, such as B_4C[81-84]. It is believed that the solid-state sintering mechanism occurs by boron substituting for silicon in the SiC lattice, creating defects in the structure which enhances volume diffusion. The role of the carbon in the densification is that it removes the SiO_2 in the SiC powder. The presence of boron and carbon impurities creates defects in the silicon carbide structure, which also enhances volume diffusion. Excess carbon inhibits grain growth and produces an equiaxed microstructure[85].

In addition, aluminium and aluminium compounds[86,87] and beryllium and its compounds[88] can be used as additives for solid-stated sintering.

Another way to overcome the low self-diffusivity of silicon carbide and to fully densify silicon carbide is to use an additive which forms a liquid phase between the grains at the sintering temperature, called liquid-phase sintering. The liquid phase functions as a high diffusivity path for atomic transport to fill the pores. If the sintering additives, which are added to the silicon carbide to form the liquid phase are in high enough quantity so that some of these additives remain in the silicon carbide material as a secondary phase, this results in a "Liquid-Phase Sintered Silicon Carbide" material. In some cases the liquid-phases disappear before the completion of the sintering, either by incorporation into the solid phase to produce a solid solution (e.g. Si_3N_4 (Al_2O_3-AlN), by crystallisation of the liquid phase, or by evaporation. This is known as transient liquid-phase sintering. This type of sintering occurs in two stages, firstly transient liquid phase sintering and then solid state sintering. Since the liquid phase is only present during the sintering and does not remain in the material as a secondary phase, this type of material is still classified as a solid state sintered "monolithic" silicon carbide material. An example of this is the sintering of Al/C doped[89] or Al_2O_3-doped[87] silicon carbide powders.

Pressure application can also enhance densification in solid-state sintering and liquid-phase sintering without affecting the rate of coarsening[77].

In solid state sintering the rate of grain boundary diffusion depends on the grain boundary diffusion coefficient, D_{gb}, and the grain boundary thickness, δ_{gb}. In liquid phase sintering, the rate of mass transfer is determined by the diffusion coefficient, D_L, of the solute atoms in the liquid phase and the thickness of the liquid bridge, δ_L, which is typically much bigger than δ_{gb}[90].

The advantage of liquid-phase sintering in SiC over solid state sintering is the former occurs at relatively lower temperatures (about 1800°C-1900°) whereas the latter requires temperatures of 2000°C-2100°C. This is an advantage since production costs are reduced and lower densification temperature also means a lower rate of grain growth, i.e. a finer, dense microstructure can be achieved. This is an advantage since a finer grain size results in a material with higher hardness, strength and wear resistance.

The main difference between the SSiC microstructure (Figure 2.11) and the LPSSiC materials microstructures (Figure 2.5) is that the solid-state sintered materials consist of crystalline grains with a grain boundary separating them, whereas in liquid-phase sintered materials there is a secondary phase(s) at the grain boundaries. The nature and amount of liquid determines what proportion of this secondary phase in the liquid phase sintered material is continuous or positioned at the triple junctions of the grains. The monolithic microstructure in SSiC, results in predominantly transgranular fracture, which results in a very low fracture toughness, reducing its usage as an engineering material. The strength and toughness of LPSSiC is significantly higher than SSiC because sintering additives and residual intergranular grain boundary phase after sintering provide toughening mechanisms. Table 2.1 shows the differences in properties between the SSiC and LPSSiC materials.

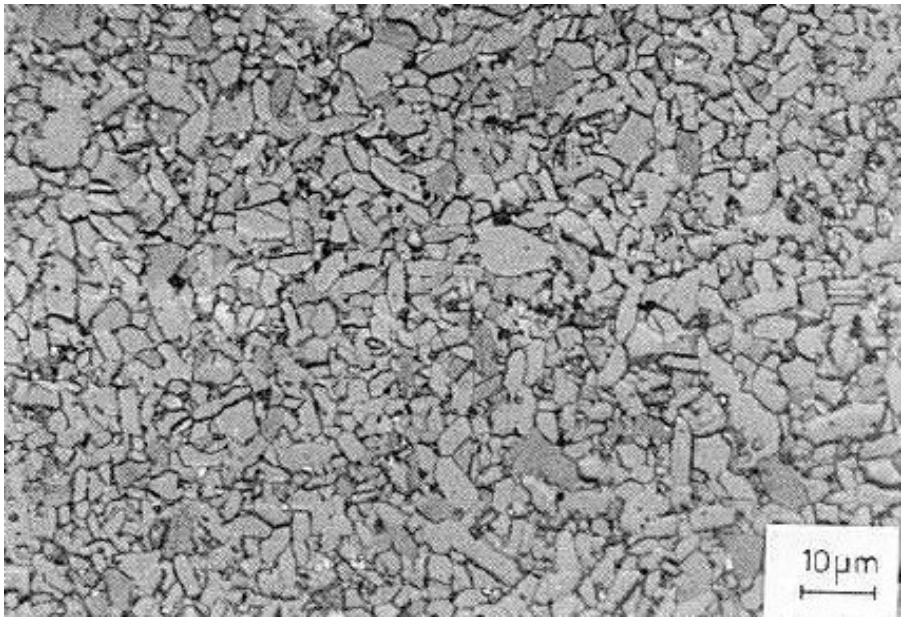


Figure 2.11 Microstructure of Solid-state sintered silicon carbide material[4].

The presence of the secondary phase in the LPSSiC materials can be a disadvantage- particularly when this remaining phase is a glassy intergranular phase which reduces high temperature mechanical properties such as hardness, strength, creep and fatigue resistance[90]

2.5 Densification methods of silicon carbide

Sintering mechanisms can be divided into solid-state and liquid-phase diffusion mechanisms. As discussed in section 2.4, for sintering and consequent densification to occur high temperatures are required. In some cases, as in the case of the covalent silicon nitride and silicon carbide ceramics, sintering additives are also required for these materials to be fully densified. Pressure can also be applied to provide an extra driving force for sintering, which can also help lower sintering temperatures. In this section, firstly pressureless sintering, and then the different types of pressure-densification techniques will be briefly discussed.

2.5.1 Pressureless sintering

The high strength covalency bonds and low self-diffusion coefficient, make it impossible to pressureless sinter silicon carbide without any sintering additives.

The main advantage of this sintering technique over other techniques is that because the samples are sintered with no mechanical application of pressure, in principle, any shape and a wide range of sizes can be sintered without having to change die design (as needs to be done in mechanical pressure sintering processes). There are however also disadvantages to not having the application of mechanical pressure. Firstly, densification is more difficult and secondly, decomposition reactions result in significant mass loss during sintering, and inadequate and irreproducible densification.

These decomposition reactions are always observed when sintering with oxide additives, mainly due to decomposition of Al_2O_3 and SiO_2. However, they are particularly a problem when no pressure is applied in the sintering, because without pressure higher temperatures and longer sintering times are required. These reactions will be discussed in greater detail in section 2.6.3.

Some researchers[10,40,91,92] have claimed that using a powder bed consisting of a mixture of coarse Al_2O_3 and SiC powder helps to improve densification in pressureless sintering. These results could not always be reproduced by other workers[10, 93, 94, 95].

Winn *et al.*[96] liquid-phase sintered α-SiC with both YAG and Y_2O_3:Al_2O_3 to form the YAG composition. They found that adding Al_2O_3 to a coarse SiC powder bed improved the densification from 92 % to 98%, claiming that it was due to diffusion of Al_2O_3 into the samples. They suggested that

the powder bed functioned by ensuring that the partial pressure of SiO and Si, within the sample was high enough "to allow reaction between them and the volatile sub-oxides of yttrium and aluminium, forming a liquid phase"[96]. They found a metallic surface on the samples sintered for 4 hours (at up to 1950^{o}C). Yttrium, silicon and aluminium rich regions were found to form these metallic layers. They also observed, some segregation of liquid phase to the surface of the sample, which was previously observed and used to enhance oxidation resistance of silicon carbide[97]. They suggested that the observed segregation of silicate to the surface of the samples was because the equilibrium thickness of silica between SiC grains was calculated to be negligible[98].

Pujar *et al.*[99] also pressureless sintered LPSSiC, using Y_2O_3: Al_2O_3 sintering additive system in a powder bed in an attempt to reduce decomposition. They found that an optimum amount of Al_2O_3 in the packing bed is important for consistent, near-full densification with negligible mass loss, and that a liquid phase richer in Al (compared with YAG) had lower porosity. Additionally, they found that the porosity was lowest when excess Al came from the powder bed via vapour transport. They concluded that a higher Al_2O_3 content with respect to YAG improved densification. They also concluded that the composition of the powder – bed influences the volatilisation of easily vaporised elements or compounds, which influences the liquid-phase composition during sintering, which will in turn influence the densification behaviour.

SiC compacts, containing 7.5 mass-% eutectic composition of Y_2O_3-Al_2O_3 system, was pressureless sintered in an Ar atmosphere by Grande *et al.*[9]. They also made use of a SiC and a SiC-Al_2O_3 powder bed. Mass loss of 1 – 11% was observed. The authors concluded that high mass loss, and not inhomogeneity in the green material, was the cause for large-scale segregation observed in the materials after heat treatment.

They also concluded that with extended heat treatment times, YAG decomposed giving rise to more yttria-rich phases. When they heat treated at 1820^{o}C for longer than 10 minutes, they found that the YAG completely decomposed leaving only yttria-rich phases. They did not report what these yttria-rich phases were[9].

Using powder beds to improve densification is however not ideal, since the composition of the powder affects the composition of the grain boundary phase of the LPSSiC material being sintered. The powder has a bad thermal conductivity, making the sintering difficult in larger furnaces. This means controlling the composition of the LPSSiC material becomes even more difficult, and it is also difficult to measure mass loss, since powder from the powder bed sticks to samples. Mulla *et al.* [100] and Ihle *et al.*[101,102,103] found that using a small CO partial pressure helped reduced decomposition reactions during pressureless sintering in the SiC-Al_2O_3-Y_2O_3 system. This is discussed in section 2.6.3.

2.5.2 Hot Pressing (HP)

During hot pressing, mechanical pressure provides an increased driving force for densification so that better densification is achieved, because it increases the rearrangement of the particles. At higher densities the mechanical pressure also acts against the internal pore pressure (P_i), helping to reduce porosity, without increasing the driving force for coarsening (grain growth).

For this reason pressure sintering can be used to sinter highly covalent ceramics such as silicon nitride and silicon carbide (even with small amounts of sintering aids)[104]. However, because of high production costs, hot pressing is not commonly used for production of SiC.

Improving the densification rate, means that sintering with applied

pressure allows for densification at lower temperatures and/or at lower sintering times. This means that, in general, hot pressing can be used to make the finest microstructures, with improved mechanical properties[105].The disadvantage of hot pressing is the high production costs (mostly due to high maintenance costs of the dies), and for this reason it is only used to produce high cost ceramics, where high density is needed. Another disadvantage of hot pressing, is that sintering is limited to simple shapes and there are also size limitations.

In uniaxial hot pressing, pressure is applied uniaxially to the powder or compressed powder (green body) in a refractory die. Pure silicon carbide, without any sintering additives, does not have a high enough plastic deformation behaviour up to its decomposition temperature and therefore can only be sintered under diamond synthesis conditions 935 kbar, 2300^{o}C) up to its theoretical density[106]. During hot pressing the pressure is limited to the strength of the die used (commonly graphite), which is up to 50 MPa[4].

A number of groups in the literature have reported on the hot pressing of LPS SiC materials. In many of these papers the objective was to study relationships between the SiC grain size and mechanical properties, especially fracture toughness. Post–sintering heat treatment was often used in addition to the hot pressing, to adjust the SiC grain size, in order to improve fracture toughness of the HP materials[12,13,15, 66, 107,108].

The uniaxial application of pressure during hot pressing, results in anisotropic orientation of SiC platelets, and this in turn can cause anisotropy in the mechanical and wear properties of the material. Therefore, for the advantage of being able to sinter more complicated forms and obtain more isotropic materials, pressureless and gas pressure sintering should be considered.

2.5.3 Hot-Isostatic Pressing (HIP)

In hot-isostatic pressing pressure is applied isostatically by a gas. In this densification method, the green body is tightly enclosed in a glass or metal container that is sealed under vacuum and placed in a pressure vessel ("can") (similar to ultra-high pressure sintering). The can is not needed if the sample is predensified to closed porosity by conventional (pressureless) sintering. In the HIP-ing process an initial gas pressure of a few thousand psi is maintained by a compressor while the sample is heated to the sintering temperature. The gas pressure is gradually increased during the heating to a high enough value to collapse the closed porosity by using isostatic gas pressure. HIP presses can usually operate up to 2000^{o}C and up to pressures as high as 200MPa (30 000 psi). An advantage of HIP-ing compared to other pressure sintering techniques such as hot pressing, is that higher pressures can be used in HIPing compared to other techniques using externally heated dies (which cannot withstand high pressures[109].

Another advantage of HIP-ing over hot pressing is that more complex shape parts can be densified with the aid of HIP-ing, for example, the HIP-ing by Jeong *et al.*[110].

Falk[111] found that during HIP-ing of SiC with a $3Y_2O_3$:$5Al_2O_3$ sintering additive system at 1800^{o}C, compared to pressureless sintering of this system at 1880^{o}C, that there was a difference in the microstructure formation. HIP-ing produced a material, which contained yttrium silicates and graphite, which was not found in the corresponding pressureless sintered materials.

In the case of solid-state sintering with boron and carbon additives, conventional (pressureless sintering) requires high temperatures and long sintering times to densify the materials. Vassen *et al.*[112] for example,

showed that using HIP-ing enabled to densification of the SSiC materials at temperatures below 1700^{o}C, using pressures up to 350MPa. This also resulted in the formation of solid-state sintered materials with smaller grain size (150 nm). Lower grain size, in general, improves the mechanical properties of sintered materials.

2.5.4 Gas Pressure Sintering (GPS)

The gas pressure sintering technique is similar to HIP-ing in the sense that the sintering process is divided into two steps- there is an initial sintering step in which the sample is sintered until there is only closed porosity. Then the gas pressure is increased to counter the pressure inside the pores to make them smaller and ideally vanish. The difference between the HIP-ing and the GPS is that the pressure used in GPS is lower than that used in HIP-ing. In GPS gas pressures are between 0.1MPa and 10 MPa, whereas in HIP-ing gas pressures range between 10 and 200MPa. The advantage of gas pressure sintering over hot pressing is that a wider range of shapes can be gas pressure sintered. A summary of the main differences between hot pressing and gas pressure sintering is given in Table 2.2.

Table 2.2 Summary of main differences between hot pressing and gas pressure sintering

Hot pressing	**Gas Pressure sintering**
(a)- sintering of uniaxially cold pressed pills	- sintering of cold isostatically pressed pills
(b)- uniaxial pressure – anisotropy expected in microstructure	- isostatic gas pressure applied to sample during sintering - more isotropic material expected
(c)- higher pressures used during sintering (30 – 40 MPa)	- lower pressures used (maximum 10MPa)
(d)- constant (high) pressure used from beginning to end of sintering procedure	- low gas pressure used until no open porosity, then gas pressure increased
(e)- as result of (d) sintering time shorter - result of this is less grain growth and decomposition	- sintering time longer - more grain growth and decomposition

Because of the longer sintering time (compared to hot pressing) the decomposition reactions discussed in section 2.6.3, are also a significant problem in gas pressure sintering.

Hue *et al.*[113] gas pressure sintered SiC-Al_2O_3 composites at 1800^oC for 2 hours, under different conditions. They found that the gas pressure compared to pressureless sintering, helped to reduce the open porosity in the sintered material. In gas pressure sintering experiments they concluded that sintering with an alumina powder bed was most effective in producing higher density and lower mass loss. Densities up to 95% of theoretical were reached[113].

Samanta *et al.*[114] did gas pressure sintering experiments (in argon under 6.33 bar gas pressure) on SiC sintered with hydroxyhydrogel powder precursors to make YAG, and solid-state mixing of Y_2O_3 and Al_2O_3 to make YAG. These samples were sintered between 1700^oC and 1950^oC by gas pressure sintering for 30 minutes in Ar atmosphere. XRD analysis showed that the formation of YAG started at 1200^oC, and increased with increasing temperature. With the correct starting mol ratio of Y_2O_3: Al_2O_3, sintering at 1400^oC, there was no residual Y_2O_3 or Al_2O_3- only YAG and SiC in the 30 mass-% YAG material. In the samples which contained more than 80% SiC, trace amounts of Al_2O_3 was detected after heat treatment at 1400^oC. The authors[114] claimed that this might be due to dilution of Y_2O_3- Al_2O_3 in the system retarding the reaction between the Y_2O_3 and Al_2O_3.

Samanta *et al.* [114] also found that in the SiC samples, which were prepared from solid-state mixing of Y_2O_3 and Al_2O_3 powders, YAG only formed at 1400^oC and large amounts of free Y_2O_3 and Al_2O_3 remained. This would imply that the powder precursor method is more effective in terms of YAG formation. Heat treatments from 1400^oC to 1950^oC yielded silicon, carbon, yttrium and aluminium monoxides, which reacted further to

form aluminium and silicon carbides, and carbon. Decomposition reactions of SiC systems with YAG are summarised in section 2.6.3.

In the solid-state mixed SiC-Y_2O_3-Al_2O_3 system materials, Samanta *et al.*[114] found that in the materials containing more than 15 mass-% YAG, mass loss increased to a maximum at 1850°C and subsequently decreased during heat treatment at 1950°C. Their explanation was that decomposition dominated over sintering at 1850°C, whereas sintering of specimens at 1950°C partially suppressed the decomposition reactions. They suggested that samples containing less than 15 mass-% YAG, where a continuous increase in mass loss was observed up to 1950°C. This might be due to insufficient liquid phase to suppress decomposition at 1950°C .They concluded that sintering included solid-state sintering phenomena, followed by liquid-phase sintering[114].

In other work by Samanta *et al.*[115], they compared three routes of processing LPSSiC: hydrodoxyhydrogel powder precursors and mechanically mixed SiC and YAG. In all the systems SiC and YAG were the major phases present, with moderate amounts of $AlYO_3$. Varying amounts of Al_4O_4C and Al_2OC together with traces of SiO_2 were also found. The presence of these phases in the gas pressure sintered materials and the mass loss, the authors attributed to a series of three possible groups of chemical reactions occurring between 1400°C and 1950°C[9, 116]. These reactions will be shown and discussed in section 2.6.3.

Samanta *et al.*[115] found that hydroxylhydrogel precursor powder preparation was better than mechanical mixing and that the preforming of YAG at 1400°C caused a reduction in mass loss, because of the higher stability of the YAG phase. In the experiments with the finer SiC powders, mass gain, instead of mass loss, was observed. They claimed that this mass gain was possible by reaction (2.3) which seemed to be favoured

with the finer SiC powder. This reaction is fact leads to mass loss and not mass gain. Trace amounts of aluminium oxycarbides in the materials, was evidence for the probability that this reaction indeed could take place in the materials.

$$Y_3Al_5O_{12} + 3C \leftrightarrow 3\,AlYO_3 + Al_2OC + 2CO. \qquad (2.3)$$

Overall mass losses were small, and increased with an increasing amount of sintering additive, which can be accounted for by an increase in decomposition reactions. They claimed that alternatively, a corresponding lower mass gain by reaction 2.3 could account for an increase in mass. Maintaining a gas pressure (of 6.33 bar in this case), as well as the pre-forming of YAG, helped to suppress decomposition reactions[115].

A few groups have published work on the gas pressure sintering of SiC with aluminium nitride-related additives. Mandal *et al.* (2001)[117] gas pressure sintered β-SiC with 10 – 55 mass-% γ-AlON, using a nitrogen and argon gas pressure of 6 bar. Mass loss during gas pressure sintering in argon was found to be higher (up to 10.75 mass-%) than when sintering under nitrogen overpressure (mass loss up to 5.5 mass-%). XRD studies and other properties indicated a solid-solution formation between SiC and γ-AlON. The mechanism of densification was proposed to most likely be solid-state molecular/ ionic movement. In the material gas pressure sintered in a N_2 atmosphere, the cubic solid solution was identified as the main phase. The materials, gas pressure sintered in argon, favoured a hexagonal solid solution as a major phase. They measured Vickers hardness of the different materials and observed a maximum hardness at 40 mass-% γ-AlON.

Mandal *et al.* (2002)[118] also gas pressure sintered SiC with 5 – 25 mass-% AlN between 1700 and 1950°C under a nitrogen pressure of 6 bar (at final sintering temperature). Analysis of XRD data revealed that a solid

solution of SiC and AlN had formed in the intergranular region. This, together with the observed SiC polytypic transformation led to the conclusion that the sintering was primarily diffusion controlled[118].

Rixecker *et al.*[119] and Biswas *et al.*[120] liquid phase sintered SiC materials by pressureless sintering (0.1 MPa of N_2) and gas pressure sintering (0.2-10MPa) with the Y_2O_3-AlN sintering additive system. In their work they showed that fully dense materials could be obtained without use of a powder bed; instead they made use of a nitrogen overpressure (0.2 - 10MPa) to inhibit the decomposition reaction of AlN (equation 2.13). They did gas pressure sintering experiments varying the α-SiC: β-SiC mass ratios, to obtain platelet strengthened microstructures showing enhanced fracture toughness.

2.5.5 Ultra-High Pressure Sintering (UHP)

In the literature, there are only four papers reporting ultra-high pressure sintering of silicon carbide. In the work by Gadzira *et al.*[22,23] (1998) and Gadzyra *et al.*[24] (2001) ultra-high pressure sintering was used to sinter SiC-C solid solutions to form superhard materials. They first produced silicon carbide powder by self-propagating high temperature synthesis using Si and graphite, and then sintered the resulting β-SiC powder with an excess of C, to allow for precipitation strengthening of the β-SiC material by formation of nanocrystalline diamond under ultra-high pressure sintering conditions.

In the work by Gadzira *et al.*[22] ultra-high pressure sintering of the synthesized powders took place at 4 GPa, at 1400^{o}C and 6GPa at 1800^{o}C both for 60 seconds. In other work by Gadzira *et al.*[23] they sintered under 8GPa, 2300^{o}C, for 90 seconds. Gadzyra *et al.*[24] ultra-high pressure sintered synthesized SiC powders between 4 and 8 GPa, between 1000^{o}C and 1400^{o}C, and 30 to 60 seconds.

Gadzira *et al.*[22] showed that unequilibrium β-SiC powders, which have a lower lattice parameter value, could be produced by interaction of fine silicon with natural exfoliated graphite, in argon at temperatures up to 1200°C. They[22] found that the SiC-C solid solution disintegrated during sintering under higher pressure (6GPa) and temperature (1800°C), with an increase in lattice parameter corresponding to a decrease in hardness.

Gadzira *et al.*[23] obtained a defect-free β-SiC structure by sintering under high pressure and temperature. Raman spectroscopy revealed the presence of C-C sp^3 bonds, which they attributed to the presence of C-antisites in the β-SiC structure. They observed a lower lattice parameter in comparison to standard β-SiC, due to substitution of C atoms for Si in the SiC lattice (i.e. solid solution formation).

Gadzyra *et al.*[24] concluded that polycrystals based on the SiC-C solid solution are much harder than polycrystals of equilibrium silicon carbide. Hardness values of the SiC-C UHP solid-solution system ranged between 40 and 41 GPa (measured between 20 and 100N), compared to hardness of equilibrium SiC, which is ca. 27 GPa.

In the ultra-high pressure sintering done by Gadzira *et al.*[22,23] and Gadzyra *et al.*[24] they did not use any liquid phase sintering additives and their sintering times were very short (up to 60 seconds).

In the work of Shinoda *et al.*[121] 1 mass% B, 3.5mass% free carbon was hot isostatically pressed with SiC under ultra-high pressure of 980MPa at 1600°C. Superplasticity can be described as the tendency for a material to exhibit very large elongation in tension at elevated temperatures. This behaviour is exhibited by fine- grained polycrystalline solids. They observed the superplastic deformation of more than 140% in their materials at 1800°C, without the presence of glassy inter-granular phase.

This means that the superplasticity was due to the grain boundary sliding mechanism, which was accelerated by the segregation of boron at the grain boundary [121].

As evidence from the literature shows, there is no work documented where α-SiC is sintered with different sintering additive compositions (liquid phase sintering) under ultra-high pressure sintering conditions.

2.6 Liquid-Phase Sintering of silicon carbide

When sintering additives (commonly 4 – 15 mass%), which form a liquid phase (s) at the sintering temperature are added to the system, this is known as liquid-phase sintering. As will be discussed in section 2.6.2 the liquid facilitates particle rearrangement and enhances mass diffusion along the grain boundary. This accelerates the densification rate and grain growth. The liquid phase also produces a secondary phase (s) in the material, which can be engineered to give the liquid-phase sintered materials certain desired properties.

The most important factors, which control liquid-phase sintering of SiC are[13,38,111, 122]:

- the specific surface area of the SiC powder
- the sintering atmosphere - Ar is the most favourable option
- the amount and composition of the sintering additives
- the sintering time
- the sintering temperature
- the processing methods prior to firing

The different sintering additives which can be used during liquid phase sintering will be discussed in section 2.6.1. In the subsequent sections the

liquid phase sintering with the Y_2O_3-Al_2O_3 system will be focused on, with some references made to the Y_2O_3-AlN system.

2.6.1 Sintering additives

In liquid phase sintering, the sintering additive either melts or reacts with another sintering additive or the major component to form a liquid, usually eutectic. This means that in the case of ceramic systems, in which the eutectic liquid phase formation governs the effectiveness of the densification, phase diagrams are important in choosing the sintering additives, their composition and the sintering conditions (especially temperature)[123].

Silicon carbide can be liquid phase-sintered using a wide range of sintering additives. The silicon carbide can be liquid phase sintered with Al_2O_3 only[87, 100 124], or by adding a rare earth oxide to the Al_2O_3[125]. Such rare earths include Y, Sc, La, and Ce[19,20,122,126]. In addition to these systems, silicon carbide can also be liquid phase sintered using the Y_2O_3-AlN system[119,120,127,128]. The most commonly used systems are the Y_2O_3-Al_2O_3 and the Y_2O_3-AlN systems, or derivatives of these systems, such as YAG[41].

Other sintering additives that are used are MgO and Al_2O_3[129], and Sialon[130]. Recently, Huang *et al.*[131] experimented with a new sintering additive system. They compared the use of sintering additives comprising $Mg(NO_3)_2$, Al $(NO_3)_3$ and $Y(NO_3)_3$ to use of additive comprising the oxide forms of these powders, MgO, Al_2O_3 and Y_2O_3, in hot pressing experiments at 1800^oC, 25 MPa pressure. Their results showed that relative density was higher when using the nitrate salts. YAG was detected by XRD in the nitrate salt derived materials, but not in the oxide-derived materials.

An important advantage of using the Y_2O_3 and Al_2O_3-system is that the additives often react to form YAG, which has been found to improve the fracture toughness of LPSSiC ceramics[10,11,132,133]. In LPSSiC materials, typically 5 – 15 mass-% of the Y_2O_3-Al_2O_3 additive system is commonly used. It was reported[134] that the sintering rate increased with increasing amount of sintering additives in the Y_2O_3-Al_2O_3 system.

The sintering temperatures used for the Y_2O_3-Al_2O_3 system are lower in Ar than in N_2 atmosphere. This results in less grain growth in Ar-sintered samples and there is also more mass-loss when sintering in N_2, which makes Ar a more favourable gas atmosphere to sinter in[135].

In the Y_2O_3-AlN sintering additives system, sintering in N_2 is in general favoured over sintering in Ar, because the N_2 overpressure effectively suppresses the decomposition reaction, (2.4) below. The N_2 overpressure improves the sintering activity, by reducing mass loss of the material[45,136].

$$2AlN \rightarrow 2Al\ (l) + N_2\ (g). \qquad (2.4)$$

However, mass loss by sintering in N_2 atmosphere in the Y_2O_3: AlN binder system is not completely avoided because the decomposition reactions:

$$SiC + 2SiO_2 \leftrightarrow 3SiO + CO. \qquad (2.5)$$
$$2SiC + SiO_2 \leftrightarrow 3Si + 2\ CO. \qquad (2.6)$$

still take place under these conditions[127].

Virkar *et al.*[137] proposed “alloying” of SiC and AlON as these are compatible phases. The β-SiC and γ- AlON can form a solid solution because of their similar crystal structures and the high reactivity of γ-AlON. Not much work on such LPSSiC ceramic systems has been reported in the literature[137,138].

SiC and AlN form a series of solid solutions in a wide range of compositions[139]. It is fairly well-understood that the AlN goes into solid solution in α-SiC in large proportion[140]. It has been found that only 1-2 %AlN dissolves in β-SiC[141]. Evidence that the AlN reacts with the SiC, causing 2H formation was given[140,141]. It was estimated that β-SiC → 2H at 1600^{o}C, 2H → 4H at 1800^{o}C and 4H → 6H at 2000^{o}C[140]. This means that under normal LPSSiC sintering conditions, the main SiC polytype composition is expected to be 4H and 6H.

The SiC-AlN phase diagram[140] indicates the formation of a metastable β-SiC phase, denoted as β'-SiC, between 1600^{o}C and 1800^{o}C. β'-SiC phase has a large proportion of hexagonal- type sites, thought to be responsible for the solubility of AlN in SiC[142,143]. The existence of SiC-AlN solid solutions was shown with SiC present as 3C and AlN as hexagonal 2H phases[144,145]. XRD phase analysis revealed that above 30% AlN the solid solution was hexagonal-2H [141].

Alkoxides or inorganic salts can be used as starting materials for the preparation of sintering aids. For example inorganic salts can be used to prepare sintering aids by the homogeneous precipitation method. The problem of coalescence in this preparation method can be prevented by using a dilute dispersion or by adding surfactants[114].

In addition to mechanical mixing of sintering additive powders, work has also been done using other powder precursor methods. For example, as discussed in section 2.5.4, Samanta *et al.*[114,115] did gas pressure sintering experiments (in argon under 6.33 bar gas pressure) on hydroxyhydrogel powder precursors to make YAG.

2.6.2 Sintering mechanism

Liquid phase sintering consists of three stages as one approaches the sintering temperature. When chemical reactions between the solid and liquid are weak, then the interfacial energies tend to dominate the rate of sintering. In this case, liquid phase sintering proceeds in different steps, as illustrated in Figure 2.12:

1) redistribution of the liquid and rearrangement of the solid particles under capillary stress gradients
2) solution-reprecipitation resulting in densification and grain-shape accommodation
3) final-stage sintering driven by residual porosity in the liquid

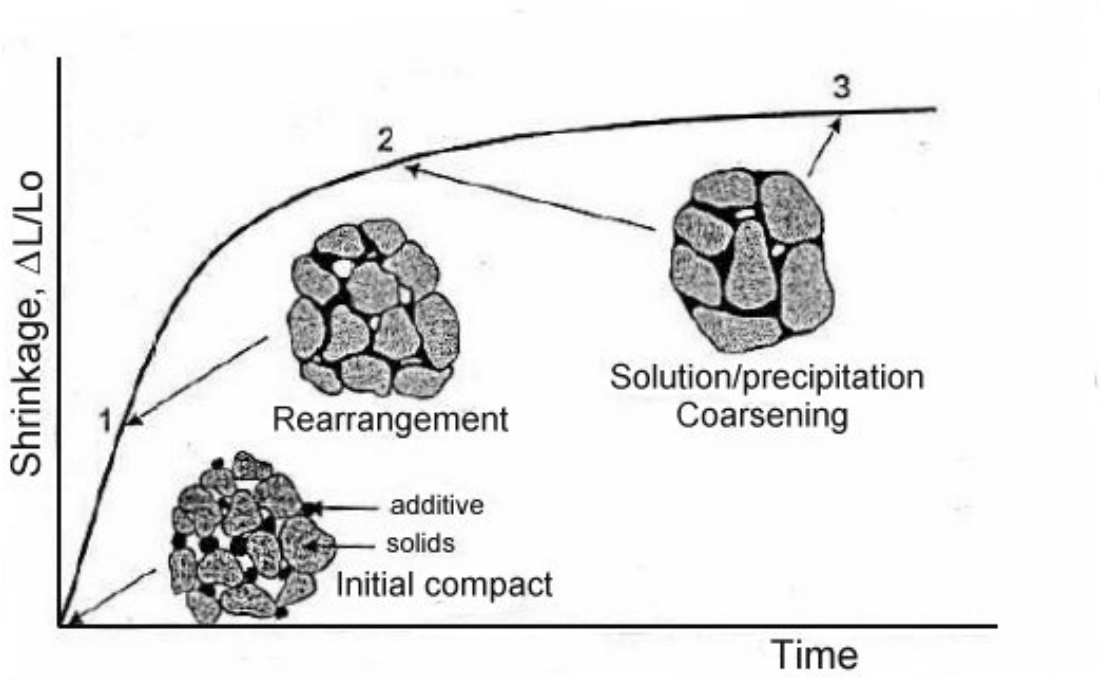


Figure 2.12 Stages of liquid phase sintering[123]

For successful liquid phase sintering, good wetting of the solute particles by the liquid is also essential. In general liquids with low surface tension readily wet solids (with low contact angle), whereas liquids with high surface tension tend towards poor wetting (with high contact angle.) If

cohesion between liquid particles is better than adhesion between solid and liquid, the liquid will not wet the solid[123].

If there is liquid formation and if there is good wetting between the liquid and solids, then surface tension forces facilitate particle rearrangement. Capillary stresses cause distribution of the liquid between particles and inside pores, to increase favourable particle rearrangement. Since in most technical silicon carbide ceramics, the amount of liquid phase is not high enough to fill all the pores, other mechanisms play more important roles in full densification. If the solid is soluble in the liquid, then the solid grains will dissolve at the solid-liquid interfaces (at the “sintering necks”) with higher chemical potential, diffuse through the liquid and precipitate on other grains with lower chemical potential.

During the solution-reprecipitation process, grain coarsening and grain shape changes take place. During the third stage of liquid-phase sintering, densification slows down because of larger diffusion distances between the now larger grains, and Ostwald ripening is dominant. Ostwald ripening is dominated by the solution-reprecipitation sintering mechanism[146], in which small silicon carbide grains dissolve in the liquid inter-granular phase and reprecipitate on larger SiC grains when saturation of the melt is reached, coarsening the structure further[147].

Therefore the overall dominating sintering mechanism during liquid phase sintering is the solution-diffusion reprecipitation mechanism[146]. This means that for successful liquid phase sintering (leading to densification) good solubility of the solid in the liquid phase is required. Good solubility of the liquid in the solid should be avoided, since this leads to transient liquid phase sintering and subsequent swelling of the compact takes place[123].

Sigl and Kleebe[41], as well as Ye *et al.*[148] confirmed that the sintering in the SiC-YAG system is controlled by the solution-precipitation mechanism.

2.6.3 Decomposition reactions observed in the Y_2O_3-Al_2O_3 system

The decomposition reactions during sintering of SiC with Al_2O_3 and the Y_2O_3-Al_2O_3 systems, are well –documented in the literature[9,100,101,102,103,149 - 154]. When sintering SiC with the Y_2O_3-Al_2O_3 sintering additive system, there are three main decomposition reactions reported in the literature[155], given in equations (2.7) – (2.9). The liquid phase sintering of SiC in Ar is influenced by the phase relations between SiC and the sintering additives (eg. yttria and alumina), by the extent of wetting of the silicon carbide grains, by the liquid phase and also by the solubility of the SiC in the liquid phase. A layer of SiO_2 coats the surface of the SiC powder particles. Decomposition reactions take place between the surface SiO_2 and SiC at the sintering temperatures, which results in mass loss. High temperature decomposition reactions which are known to occur in LPSSiC materials (with the Y_2O_3-Al_2O_3 sintering additives system) are given in equations 2.7 – 2.21.

During high temperature sintering, reactions can also take place in which SiC and YAG react with CO in the furnace atmosphere. Transport of Al_2O_3 from a powder bed, into the samples is often reported[111] and understood to happen by vapour phase transport in the form of Al_2O and AlO[9,92]. This results in mass gain in the materials. The overall mass loss or gain measured after pressureless sintering, gas pressure sintering and/ or heat treatments is the result of reactions (2.7) - (2.15). The net result of the Al_2O_3 transport depends on the sintering conditions and composition of the materials[154,115].

- Group 1:

  $SiC + 2\ SiO_2 \leftrightarrow 3SiO + CO,$ (2.7)

  $SiC + Al_2O_3 \leftrightarrow Al_2O + SiO + CO,$ (2.8)

  $SiC + Y_2O_3 \leftrightarrow Y_2O + SiO + CO.$ (2.9)

- Group 2:

$$SiO + 2C \leftrightarrow SiC + CO, \quad (2.10)$$

$$Al_2O + 3C \leftrightarrow Al_4C_3 + 2CO, \quad (2.11)$$

$$SiC + CO \leftrightarrow 2C + SiO. \quad (2.12)$$

- Group 3:

$$Y_3Al_5O_{12} + C \leftrightarrow 3AlYO_3 + 2AlO + CO, \quad (2.13)$$

$$Y_3Al_5O_{12} + 2C \leftrightarrow 3\ AlYO_3 + Al_2O + 2CO, \quad (2.14)$$

$$Y_3Al_5O_{12} + 3C \leftrightarrow 3\ AlYO_3 + Al_2OC + 2CO. \quad (2.15)$$

Decomposition reactions during pressureless sintering (and gas pressure sintering) result in material leaving the samples in the form of gases SiO, Al_2O and CO. This in general leads to a deterioration of mechanical properties of the materials. At temperatures above 1850°C, authors[100] expected the vapour pressures of Al and Si in reactions 2.16 and 2.17 to increase.

$$2SiC + Al_2O_3 \rightarrow 2Si + 2Al_2O + 2CO. \quad (2.16)$$

$$3SiC + Al_2O_3 \rightarrow 3Si + 2Al + 3CO. \quad (2.17)$$

Mulla *et al.*[100] found that as they increased the amount of Al_2O_3 in the green compact from 5 to 30 mass-%, the amount of Si detected in the sintered samples increased from 0.2 – 1.5 mass-%.

Thermodynamic calculations and experimental work by Mulla *et al.*[124], Misra *et al.*[153] and Ihle *et al.*[101] also showed that the presence of C has a significant influence on the decomposition reactions taking place, as indicated in the reactions 2.18, 2.19 and 2.20. They found elemental Si and Al in their materials after sintering, due to these reactions.

$$Al_2O + C \rightarrow 2Al + CO. \quad (2.18)$$

$$SiO + C \rightarrow Si + CO. \quad (2.19)$$

$$SiO + 2C \rightarrow SiC + CO. \quad (2.20)$$

Thermodynamic data for the decomposition reaction calculations can be found in Table 3 in reference 113.

In the case of hot pressing these decomposition reactions only take place to a very limited extent, at the surface between the silicon carbide grains and silica, by reaction 2.7. This is because all of the above reactions take place during the densification stages in the sintering, and the densification rate in hot pressing is very high. Compared with pressureless sintering and gas pressure sintering, there is less time for evaporation[38,122].

In the case of gas pressure sintering, because only a very low pressure is maintained until the sample is 95% dense, there is more time for decomposition compared to hot pressing. This makes the gas pressure sintering a more difficult processing technique, less likely to be successful. Not all materials that can be fully densified by hot pressing, can be fully densified by gas pressure sintering.

Yttria does not show any significant gas phase reactions with silicon carbide[9,45,156], nor does it by itself form enough melt phase to allow for densification below 2000°C. Baud *et al.*[150] confirmed that the decomposition of a SiC-Al_2O_3-Y_2O_3 system is similar to decomposition observed in the SiC-Al_2O_3 system. Thermodynamic calculations by Baud *et al.*[150] show that gaseous CO, SiO, Al_2O and Al are the main species in the atmosphere during sintering of both these systems.

Mulla *et al.*[100,124] found that mass loss during pressureless sintering of β-SiC with Al_2O_3, can be reduced by a factor of 2 - 4, by sintering in a pressurised CO atmosphere (0.105 MPa pressure), instead of sintering in pure argon. They concluded that an optimum Al_2O_3 content of 10 mass-% produced a material with the highest theoretical density and also a

microstructure with more elongated grains, for *in-situ* toughening. Ihle *et al.*[101,102,103] pressureless-sintered porous LPSSiC materials, which show higher tendency towards decomposition reactions than dense LPSSiC materials. They confirmed that a mixture of Ar and CO in the sintering atmosphere, improves densification during pressureless sintering of SiC with the Y_2O_3-Al_2O_3 system.

Ihle *et al.*[103] proposed a simplified decomposition reaction, given in equation (2.21), as the most probable reaction at temperatures in the range 1950 – 2150 K in the SiC –Al_2O_3-Y_2O_3 system.

$$4SiC(s) + 2Al_2O_3\ (s,l) \rightarrow 4CO(g) + SiO(g) + Al_2O\ (g) + 0.5\ Al\ (g) + 3Si(l) + 1.5\ Al\ (l). \quad (2.21)$$

This proposed reaction by Ihle *et al.* was based on thermodynamically calculated compositions of the gas phase and liquid melt, and confirmed by sintering experiments[103].

2.6.4 Microstructure

Microstructural investigation is very important in the engineering of materials, because this gives information about the processing and how the processing must be changed to give desired properties of the material.

The microstructure of the liquid phase sintered material consists of crystalline grains and the grain boundary or “secondary” phase resulting from the liquid. The secondary phase is often a partially amorphous glassy phase. Depending on interfacial tensions, this secondary phase may penetrate between the crystalline grains, separating the grains with a layer between 1 and 5 nm thick, or they may partially separate the grain boundaries[123]. This is discussed later in this section.

The “microstructure” of the LPSSiC material, includes the phase content of the primary and secondary components, as well as the distribution of the primary and secondary phases, including the grain size and shape.

A wide variety of grain shapes, from equiaxed to elongated grains with curved or straight (faceted) sides are possible, depending on the solute and liquid composition. In systems with isotropic interfacial energies, if the amount of liquid phase is around 5 vol.-%, then the grains tend to be rounded, whereas if the amount of liquid phase is higher, then the grains tend to be spheroidal. In the cases of lower additive content, grain shape accommodation takes place, in which the grain shape changes to develop flat contact regions between neighbouring grains. This results in the most efficient packing of the grains[123].

When particulate materials are sintered and / or heat treated at high temperatures, grain growth occurs. The driving force for this grain growth is the reduction of grain boundary area, which has the highest energy component in the microstructure. Grain growth can be divided into two types: normal and “abnormal” grain growth. Normal grain growth results in a narrow distribution of grain size and shape, whereas in abnormal grain growth, a few large grains grow at the expense of the smaller grains. This often results in the grain size distribution becoming bimodal. It is possible that after a long enough heat treatment time, that the large grains impinge on each other and revert to a “normal” distribution of grains[157].

Anisotropic abnormal grain growth occurs in systems with non-isotropic interfacial energies, resulting in different growth rates in different directions of the grain. If the liquid content is high, prismatic shaped grains can be seen, whereas if the liquid content is lower, elongated grains with curved sides or plate-like grains with straight (faceted) sides may be seen[123]. Abnormal grain growth can also be as a result of the grain size distribution in the starting material. According to the Hillert theory[158] if a grain is larger

than twice the average grain size (by area), then it will grow abnormally.

For liquid phase sintering, the grain growth is related to the growth exponent in the equation[159]:

$$d^n - d^n_o = kt, \qquad (2.22)$$

where,
d^n is the mean grain size after heat treatment time t.
k is a constant and d^n_o is the initial mean grain size (before heat treatment for time t), and
n is the growth exponent which determines the growth law.

Most commonly, n = 2 for interfacial reaction control and n = 3 for diffusion control. i.e. this parameter is governed by whether interfacial reaction or diffusion is the rate determining step in the densification process[159]. However, it is not possible to determine the sintering mechanism purely from the value of the exponent.

Crystal growth theories form the basis of the general rule proposed by Lee *et al.*[160] that faceted grains imply interface-reaction controlled coarsening and rounded grains imply diffusion-controlled coarsening. This has been verified in many systems[160-164] and is considered true for LPSSiC. By virtue of the fact that the silicon carbide grains in their system were faceted and the fact that the coarsening kinetics was found to be independent of the volume of grain boundary phase present, Ye *et al.*[148] concluded that the coarsening in their LPSSiC system was interface-reaction controlled.

Much work has been presented in the literature, in terms of determining the SiC grain size (usually given as the mean), using scanning electron microscopy (SEM)[12,15,165]. In these papers[12,15,165], the focus was on

relating the grain size to mechanical properties, such as hardness, fracture toughness and strength. Much work has been done on systems in which the β to α SiC phase transformation was exploited to produce large elongated grains in the microstructure[10-14]. The sintering mechanism for liquid-phase sintering of SiC is well understood to be a solution-reprecipitation process. When sintering β-SiC there is a phase transformation, in which mainly the β-SiC grains dissolve in the liquid phase and α-SiC reprecipitates on pre-existing added α-SiC seeds. Anisotropic growth of the α-SiC grains occurs because of the hexagonal symmetry of the α-SiC, resulting in a platelet microstructure (as shown in Figure 2.6). The volume density of α-SiC seed crystals determines the extent of steric hinderance during platelet growth, and therefore as the volume of the pre-existing α-SiC grains increases, the aspect ratio of the platelets increases[42].

Lee *et al.*[42] reported on the effects of the β to α transformation on the LPSSiC microstructure. They pressureless sintered two groups of materials at 2000°C, with the $Y_3Al_5O_{12}$ (YAG)-Al_2O_3 eutectic mixture of Y_2O_3 and Al_2O_3. The findings of Lee *et al.*[42] were in agreement with Padture[10] in that although grain growth was observed in the α-SiC system after sintering for longer times, no elongated grains were observed to form. Their findings are also in agreement with Padture[10] in that when they sintered β-SiC for longer times, elongated "platelet" formation was observed.

The work by Kim *et al.*[166] contradicts the idea that the β to α transformation is needed for platelet formation. They were able to produce an elongated-platelet microstructure, when sintering β-SiC at 1850°C, which is below the temperature (1950°C) at which the β to α transformation is expected to occur. XRD results gave evidence of a small degree of β to α transformation, but Kim *et al.* concluded that the degree

of β to α transformation did not warrant the observed level of anisotropic platelet growth.

In other work by Kim *et al.*[13], they hot pressed α-SiC with 7.2 mass-% YAG and 4.8 mass-% SiO_2 at 1850°C for 1 hour, followed by a four hour heat treatment at 1950°C. They observed the formation of an elongated-platelet microstructure after heat treatment of a sample which was sintered starting from fine, pure α-SiC powders. They found that when they sintered with an α-SiC starting powder above a certain grain size, they did not obtain the same elongated α-SiC grains in the microstructure of the heat treated hot pressed material. This also contradicts the idea that the β to α transformation is required to produce a platelet-strengthened microstructure.

Baud *et al.*[165] pressureless sintered three matrix-seed SiC systems (β-α,β-β and α-α platelets) with 3 mass-% YAG- Al_2O_3 grain boundary phase at 1950, 1780, and 1930°C respectively. They then did image analysis on all the microstructures and found that grain growth of equiaxed grains was continuous, whereas grain growth of elongated grains occurred in two steps. They reported that in the β-α system, up to a certain length of time in sintering the grains first lengthen, and then in a second stage the grains predominantly thicken, with less lengthening. In the β-β system, the lengthening and thickening took place at the same time. Their results agreed with other author's work[10], in that the presence of an amount of α-SiC is important for elongated platelet formation. However, they also observed a small degree of elongation when sintering with only β-SiC (the β-β system), smaller than in the β-α system.

The relationships between these elongated-platelet microstructures with properties will be discussed in the next section, 2.6.5.

In most of the published literature on LPSSiC materials, XRD is generally used to determine the phase content of the materials. In the LPSSIC materials sintered with Y_2O_3 and Al_2O_3, the most common composition chosen is that which will yield YAG as the main phase in the grain boundary component[10,11,167] and pure YAG is used in many papers[168]. The XRD results in general indicated the presence of the different SiC polytypes (as discussed in section 2.2), showing that 6H and 4H polytypes tend to dominate over 15R and 3C polytypes[41]. The advantages of the YAG grain boundary on mechanical properties will be discussed in section 2.6.5.

Accurate quantitative phase analysis of a fine-grained microstructure is a difficult task because of the fact that the smaller the crystallite-size in a material, the broader the XRD peak. The SiC polytypes, have very similar energies/crystal structures, as a result, the degree of overlap between the XRD peaks of the different SiC polytypes is very high. These factors make separation of the phases and consequent quantitative analysis of the SiC phases in the LPSSiC material a difficult task. Few groups in the literature have successfully done Rietveld calculations to determine SiC polytype and grain boundary content in SiC based materials. Hongchao *et al.*[65] and Ortiz *et al.*[62] showed the success of the Rietveld calculation in determining SiC polytype content and that it was superior to other methods in quantitative measurement of the SiC polytypes (6H, 4H, 15R and 3C). Ortiz *et al.*[60,61,63,64] did further work in quantitative phase analysis using the Rietveld method in LPSSiC systems, where YAG was found to be the main grain boundary phase observed in their materials.

In addition to these analytical difficulties, the formation of amorphous inter-granular phases is a common problem, because usual XRD phase analysis techniques cannot detect non-crystalline phases. This problem was overcome by Ye *et al.*[127], who were able to detect N-rich amorphous intergranular phases in LPSSiC samples using wavelength dispersive

spectroscopy (WDS) on SEM images. Transmission Electron Microscopy is also used to identify amorphous phases in the LPSSiC materials[41,111].

Sigl *et al.*[41] showed that a result of the solution precipitation mechanism in LPSSiC materials, is a core-rim structure of the SiC grains, as illustrated in Figure 2.13. Using energy dispersive techniques in the SEM and TEM, they observed the presence of the Y, Al and O elements in the outer rim part of the silicon carbide grains. The presence of these elements in the SiC was not observed by Falk[111], but this may be because Sigl *et al.* sintered at a higher temperature, 1950°C, to Falk , who sintered at temperatures between 1800 and 1880°C.

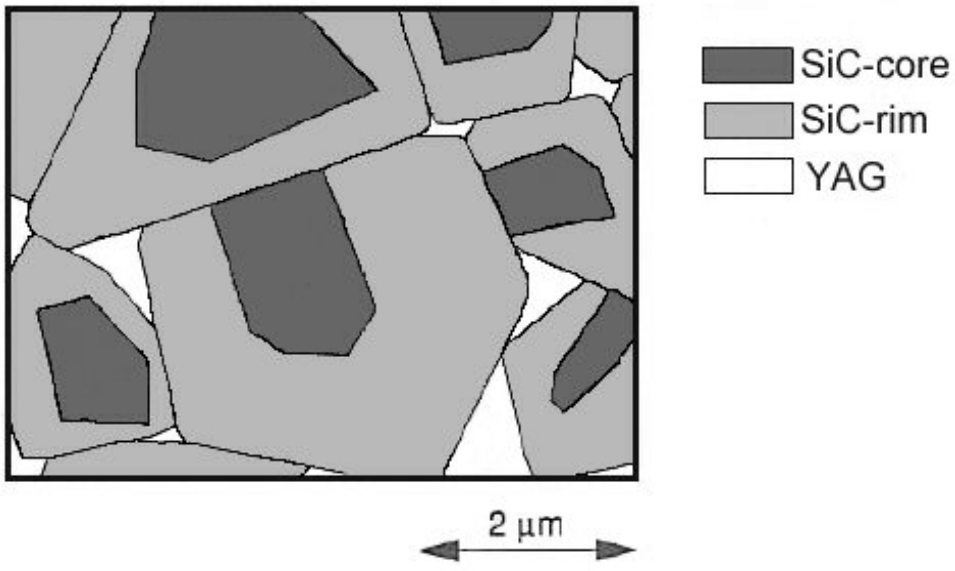


Figure 2.13 Schematic diagram of Core-rim structure as illustrated by Sigl *et al.*[41]

Core-rim structures are a well-known phenomenon observed in different materials such as $BaTiO_3$, Si_3N_4/SiAlON systems and cemented carbides/ carbonitrides. Rudiger and Exner[169] gave an explanation of the core-rim structure observed in cubic hardmetals. They suggested that mixed cubic carbides, like (W, Ti)C, which are produced at temperatures higher than

1700°C, are not in equilibrium at temperatures typically used for sintering of these carbides (ca. 1450°C). Based on experiments with (W,Ti)C crystals, they showed that diffusion only equilibrates concentration gradients above 1800°C[170]. They rejected diffusion as the mechanism for forming the core-rim structure. They then concluded that the arrangement of phases must have developed by the dissolution of non-equilibrium phases in the liquid, followed by reprecipitation of equilibrium (rim) phases onto undissolved nonequilibrium core particles.

According to Clarke[98], theoretical modelling of continuum approaches considering interfacial energies or force balance normal to the grain boundary, suggests that there is an equilibrium thickness of amorphous phase between grains in different systems[98]. The amorphous film is the result of opposing attractive van der Waals forces between grains, and repulsive forces due to the film structure. These calculations by Clarke showed that a negligible thickness of amorphous film of SiO_2 should exist between SiC grains. However, the presence of an amorphous film between SiC grains, shown in Figure 2.14, has been reported by Sigl *et al.*[41], Falk[111], Schmid *et al.*[171] and Chen *et al.*[66]. Sigl *et al.*[41] also observed amorphous films between the SiC and YAG phases, as shown in Figure 2.15. In general the films were 0.8 – 1.5 nm thick. Falk observed that Y was absent in these glassy regions, implying that crystallisation of YAG depleted the remaining liquid of Y, shifting the composition towards aluminium silicates. Since the glass phase found between the SiC grains in the Y_2O_3-Al_2O_3 LPSSiC systems, is not purely SiO_2, this does not truly contradict the calculations of Clarke in the SiC system.

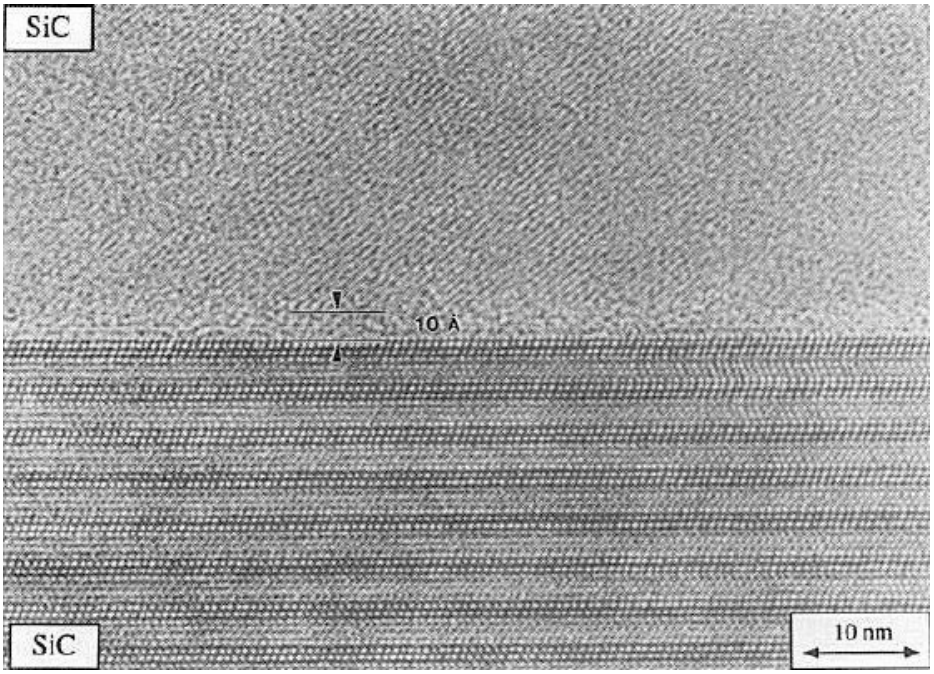


Figure 2.14 TEM micrograph showing the amorphous film between two SiC grains (indicated by the arrows, approximately 1 nm thick)[41]

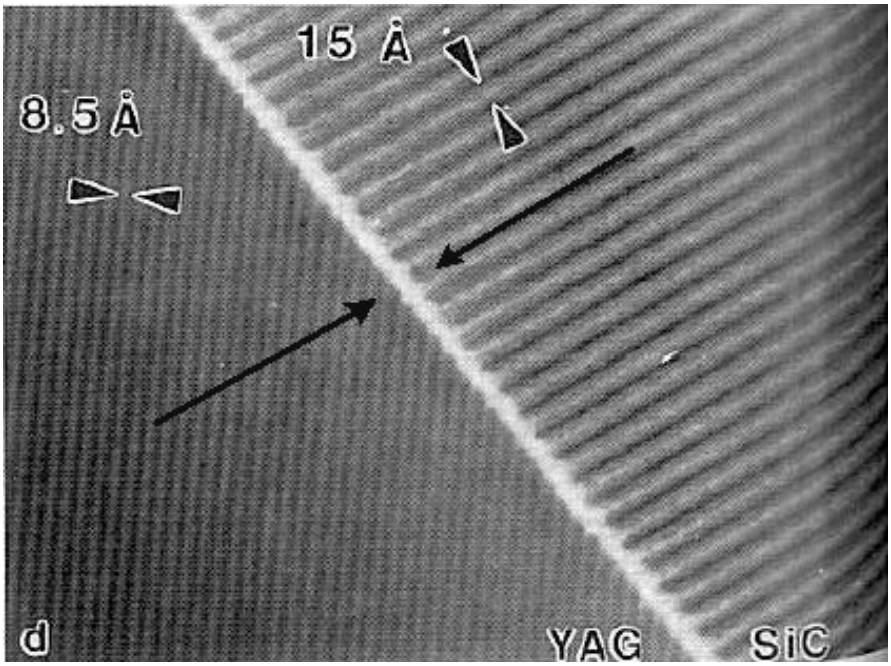


Figure 2.15 TEM micrograph showing the amorphous film observation between SiC and YAG materials[111]

According to Gröbner[172], in the Y_20_3-Al_2O_3 system there are three phases that can possibly form: $YAlO_3$ (YAP), $Y_4Al_2O_9$ (YAM) and $Y_3Al_5O_3$ (YAG). The "YAP" phase is an orthorhombically deformed Perovskite structure, which is not stable at room temperature and therefore, even if this phase forms, it can partially decompose during cooling down to room temperature. The YAG and the YAM were found to be stable. Note that Gröbner did not work on LPS SiC system in particular, as he worked on the Al_2O_3- Y_2O_3 system in general.

When the system is cooled after sintering, it is possible to see a combination of these phases (depending on the cooling rate and composition). The YAP (Yttrium Aluminium Perovskite, $YAlO_3$) phase is not stable at room temperature and therefore when analysing samples with 50mol-%Y_2O_3: 50mol%Al_2O_3, under normal cooling conditions one will expect to see the YAP phase in a mixture with YAG and YAM.

α-SiC and β-SiC convert to 6H and 4H polytypes in the presence of YAG[41,93]. One has to take into account diffusion of Y, Al[40] and O and what influence this has on stabilising particular polytypes. $YAlO_3$ formed by reactions in Group 3, in section 2.6.3 above, might decompose into YAG and $Y_{4.67}$ $(SiO_4)_3O$[114,173].

2.6.5 Microstructure- property relationships

Toughness to Structure Relationship

In ceramic materials, when stress is applied to the material there is no plastic deformation, and therefore no stress relaxation. Instead, the stresses become concentrated at flaws/ cracks in the material. The critical stress intensity factor, K_{IC}, for a material is defined to be the critical stress/ energy at a crack tip in the material, required to cause the further propagation of the crack. Fracture toughness may be defined to be the

resistance to fracture, and therefore K_{IC} is a measure of fracture toughness of a ceramic material.

The two features of the microstructure, which have the greatest influence on the mechanical (fracture toughness in particular) properties of the material are the absence/presence/composition of a grain boundary phase, and the grain sizes of the phases in the material after sintering and further heat treatments.

Figure 2.16 shows a schematic correlation between fracture toughness and critical structural features of LPSSiC.

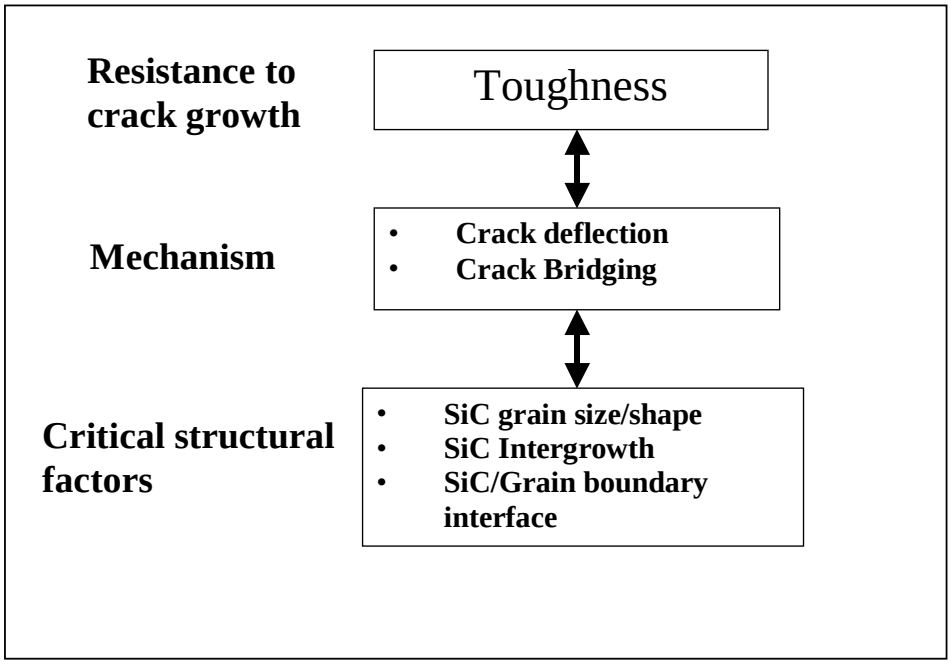


Figure 2.16 Relationship between fracture toughness and critical structural factors for LPSSiC

Strength and fracture toughness properties are higher in LPSSiC, than in SSiC because liquid phase sintering allows sintering to take place at lower temperatures, and the liquid phase improves strength by reduction of defects during sintering[10]. The presence of the secondary phase in the

LPSSiC material, allows the activation of toughening mechanisms such as crack bridging and crack deflection. This is believed to occur because of mismatch in thermal expansion between the grain boundary and the SiC phases, which places the grain boundary under residual tensile stress[174]. Interfacial debonding at the interface between the grain and grain boundary is a second mechanism for promoting intergranular fracture by weakening the grain boundary[10,175]. Both of these phenomena produce a path along the grain boundaries for the crack to propagate along. The resultant intergranular crack path results in more energy being expended than would be if the crack path were transgranular, since the intergranular path is effectively longer than the transgranular path. This toughening mechanism is known as crack deflection.

YAG in particular has been found to improve fracture toughness values [10, 11, 132,133], due to the difference in thermal expansion coefficient between SiC and YAG which is approximately 5 X 10^{-6} $^{o}C^{-1}$[10]. The presence of glassy phases in the grain boundary reduces the thermal expansion mismatch to ca. 3 X 10^{-6} $^{o}C^{-1}$. i.e. the presence of crystalline YAG is more favourable for the enhancement of toughening mechanisms, than the presence of glassy phases.

In equiaxed materials, crack deflection is known to occur. This also occurs in a bimodal microstructure, containing platelets, except that the larger grains dispersed through the material, increase the amount of crack deflection and leads to significant crack bridging toughening mechanism[10].

Crack bridging, an example of which is given in Figure 2.17, is a toughening mechanism, which develops behind the advancing crack. Crack bridging is the process of physical contact formation between the mating crack surfaces, through fibres, whiskers, platelets (elongated grains), inclusions and surface asperities, which interlock the mating crack

surfaces[176]. Padture[10] observed almost two-fold increase in fracture toughness (up to 4.0 $MPa.m^{1/2}$) when platelet formation and associated crack bridging was observed in his materials.

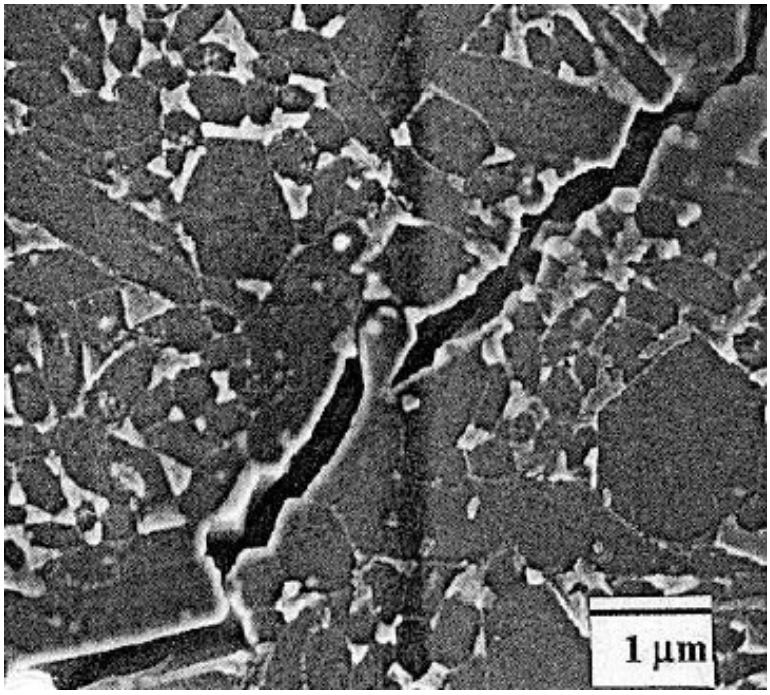


Figure 2.17 An example of crack bridging[174]

Many papers in the literature have reported relationships between silicon carbide grain size and fracture toughness[10-15,107,119,120,168]. All of these papers, with two exceptions[112 and 165], showed that an increase in aspect ratio of grains, i.e. the development of a bimodal grain size distribution increases the fracture toughness, due to factors as discussed in the above paragraph. One of these exceptions was in the work by Baud *et al.*[165], in which they did not observe increase of fracture toughness or activation of crack bridging when they obtained an elongated grain microstructure. The explanation for this by these authors was related to the method of toughness measurement, namely, indentation. The authors stated that the kinetic energy associated with the fast and unsteady growth of flaws inhibited the development of crack bridges. They found that the fracture toughness was related to the square root of d_{50}.

In most of these papers which focus on the influence of SiC grain size and aspect ratio on the toughness of the material, the β to α SiC phase transformation was exploited. The fracture toughness could be increased up to 8 $MPam^{1/2}$ with such a microstructure[119].

With the absence of silica, crystalline phases are expected to form at the triple points, because silica is a major vitrifying component. It is at present not well understood how the increase or decrease of crystallinity of the grain boundary phase affects the mechanical properties of the LPSSiC material[122]. Cheong *et al.*[108] argued that crystallization of the YAG phase reduced the aluminium content in the remaining glass phase, which caused the thermal expansion coefficient of the glass to come closer to that of the silicon carbide[177]. This might explain why Cheong *et al.* observed a decrease in fracture toughness from 3.8 $MPa.m^{1/2}$ to 3.5 $MPa.m^{1/2}$ after heat treatment for 2 hours, and no change after 4 hour heat treatment at 1950^{o}C. They did observe an increase in fracture toughness after 6 hour heat treatment (up to 5.0 $MPa/m^{1/2}$), and argued that on longer heat treatment crystallization of the more Y-rich phases, reduced the yttrium in the remaining glass, which could result in an decrease in thermal expansion mismatch between the SiC and grain boundary material again[177].

Sciti *et al.*[132] and Zhou *et al.*[178] examined the effects of different grain boundary phases on mechanical properties. Without a large platelet microstructure, Sciti *et al.* found that fracture toughness values were low (ranging between 2.68 and 3.10 $MPa.m^{1/2}$). They compared two additive systems, Y_2O_3-Al_2O_3 and Y_2O_3-La_2O_3, and observed that fracture toughness was highest in the material which contained YAG and amorphous phase in the grain boundary. Zhou *et al.*[178] hot pressed and then annealed the different sintering additives, Al_2O_3 together with La_2O_3, Nd_2O_3, Y_2O_3 and Yb_2O_3. Different microstructures were observed in the different composition materials after annealing. The fracture toughness

was found to be highest (5.5 MPa.$m^{1/2}$) in the Al_2O_3-Nd_2O_3 system material in which the aspect ratio of the grains was highest (7.0). In all of these systems though, a steady increase in fracture toughness was observed on heat treatment by forming platelets in the microstructure.

Balog *et al.*[179] hot pressed β-SiC powders with different rare-earth oxides together with AlN. They added either α- or β-SiC seeds, and sintered at 1850°C in a mixture of Ar and N_2.The rare-earth oxides they used were Y_2O_3, Yb_2O_3, Sm_2O_3. Post-sintering heat treatments were done at 1850°C. They found that addition of β-seeds hindered the β to α phase transition and resulted in an increase in the fracture toughness. The highest fracture toughness (6.5 MPa.$m^{1/2}$) was for a material doped with β-seeds, with Yb_2O_3-Sm_2O_3-AlN additives annealed for 5 hours at 1850°C. They concluded that with decrease in ionic radius of the rare earths, fracture toughness decreased. This they attributed to be due to the chemistry of the intergranular phase.

Strength to Structure Relationship

Orowan proposed a sine function to represent the stress normal to atomic planes in an ideal crystalline solid, as a function of atomic interplanar separation. He determined the parameters of the sine function by fitting it to the Young's modulus and interfacial energy of the solid[180,181]. The theoretical breaking stress of an ideal solid is the value of the stress at the maximum of the sine function assumed by Orowan[181]. i.e. it is the stress required to separate atomic planes in a pure solid.

A stress applied to a material will deform it, unless the strength of the material is exceeded, in which case the applied stress will cause the material to fail[180]. The strength of ceramic materials, which in general contain defects and dislocations, is related to the stress at which

catastrophic crack growth takes place starting at a critical flaw in the sintered material.

The Griffith equation, given as equation 2.23[132,182], gives the relationship between yielding strength and flaw size in the material.

$$\sigma = Y \frac{K_{1c}}{\sqrt{a}}, \qquad (2.23)$$

where σ = yield strength,

Y= geometric factor, which depends on the flaw shape, and

a= flaw size.

Figure 2.18 shows schematic relationship between strength and critical structural features of LPSSiC.

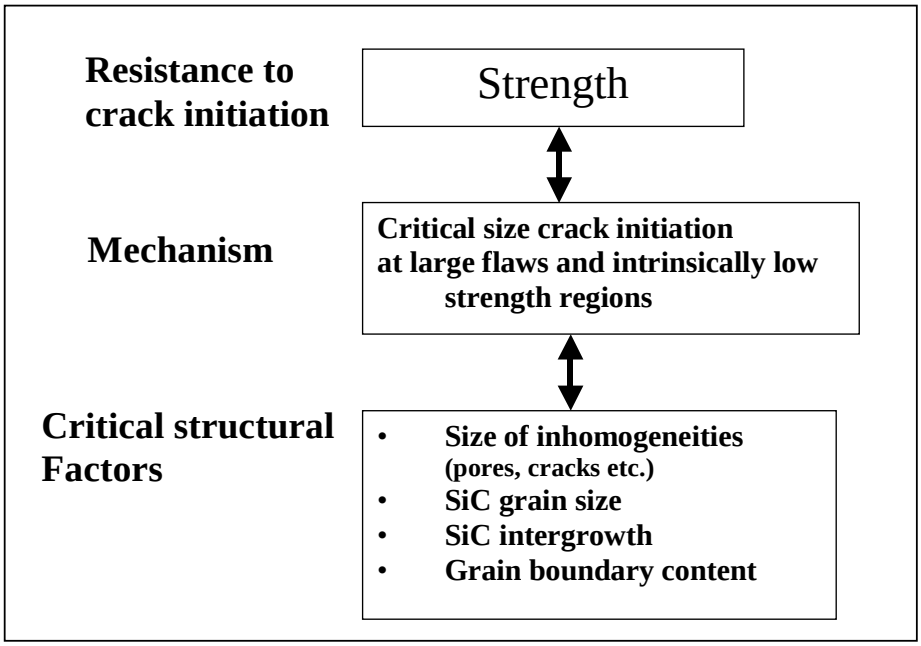


Figure 2.18 Relationship between strength and critical structural factors for LPSSiC

Studies in the literature have shown that the strength of LPSSiC materials could be increased with decrease in silicon carbide grain size. This has

been shown to be true for the Y_2O_3-AlN[120] sintering additive system, where a maximum of 636 MPa was observed in the finest grain equiaxed material. It has also been demonstrated in the Y_2O_3-Al_2O_3 system[15], where strength increased from 410 to 540 MPa after 4 hour annealing, but decreased to 460 MPa after 8 hour heat treatment, due to the coarse microstructure formation. Biswas *et al.*[120] showed that strength could also be increased from 470 MPa to 526 MPa by decreasing the grain boundary volume from 10 volume-% to 7-volume-%. The error/ standard deviation of the determined strength values, was however quite high (95MPa). In accordance with the discussion on toughening mechanisms above, an increase in strength (420 MPa to 600 MPa) with an increase in YAG, was observed by Cheong *et al.*[108].

Sintering in an atmosphere with a mixture of Ar and N_2 has the advantage of producing a material with improved flexural strength. This is because of increased densification of LPSSiC ceramic materials when sintering in increased Ar atmosphere at lower temperatures[136], and the resulting fine grain size of the material.

Biswas *et al.*[120] observed that sintering of α-SiC with Y_2O_3 and AlN, compared with „conventional“ liquid phase sintering of silicon carbide (i.e. sintering with Y_2O_3 and Al_2O_3), had the advantage of improved strength at 1200°C. Instead of a decrease in strength, as observed by Sciti *et al.*[132], they observed an increase in strength from 480 MPa at room temperature to 600 MPa at 1200°C. Biswas *et al.* attributed this increase in strength as being the result of a “concurrence” between softening of the intergranular phase in the bulk, and oxidation-induced surface strengthening[120].

Rixecker *et al.*[119], Biswas *et al.*[120] and Keppeler *et al.*[183] all observed an increase in bending strength between 1000 and 1200°C, in comparison to room temperature values followed by a decrease at 1400°C, when sintering with SiC with Y_2O_3-AlN additives. This was thought to be due to

initial softening and subsequent stress relief, by viscous flow of the grain boundary phase between 1000°C and 1200°C. Above 1400°C more softening resulted in the decrease in strength of the materials.

When liquid phase sintering with Y_2O_3-AlN, both Rixecker *et al.*[119] and Biswas *et al.*[120] observed a high strength retention up to 1400°C. Rixecker *et al.*[119] found that after heat treating the materials for 0.2 hours at 1200 – 1300°C in air, strength was observed to increase from 440 MPa in one material to above 1GPa. Biswas *et al.*[120] found that the most favourable strength behaviour up to 1400°C was for 60 vol.-% AlN in the material (i.e. a composite). Both groups[119,120] attributed this strength retention due to generation of compressive stresses by the oxidation of the intergranular oxynitride phases (forming YAG and γ-$Y_2Si_2O_7$ phase).

In the case of sintering with Y_2O_3-Al_2O_3, Magnani *et al.*[184] claimed that oxidation above 1200°C, resulted in a decrease in strength from 532 MPa at room temperature to 240 MPa at 1400°C[184]. They suggested that this was because oxidation of the SiC occured, forming SiO_2, which then reacted with YAG to form yttrium silicate, γ-$Y_2Si_2O_7$ and alumina. These reactions were detrimental to the strength because evaporation of gases resulted in bubble, and hence pore formation in the microstructures. Sciti *et al.*[132] also observed a decrease in strength at temperatures above 1200°C, where they observed a decrease in strength from 750 MPa at room temperature to below 200 MPa at 1300°C. They attributed it to be due to softening of the amorphous part of the grain boundary phase.

The effect of different additive systems on strength of hot pressed materials after post-sintering heat treatments was studied by Zhou *et al.*[178]. They hot pressed at 1800°C in Ar and then heat treated at 1850°C and 1950°C in Ar, for 3 hours. They observed that strength either increased or decreased with increase in grain size on heat treatment, depending on the sintering additives used. In the Al_2O_3-La_2O_3 and Al_2O_3-

Nd_2O_3 systems strength increased from about 500 MPa to 650MPa, and 550 to 610 MPa respectively, when heat treatment temperature increased from 1800°C to 1950°C. In the Al_2O_3-Y_2O_3 and Al_2O_3-Yb_2O_3 systems, a different trend was observed. In these systems strength increased from 580 MPa to 660 MPa, and 650 MPa to 720 MPa respectively, with increase in heat treatment temperature from 1800°C to 1850°C. A sharp decrease in strength was observed after heat treatment at 1950°C, to 440 MPa and 370 MPa, for the Al_2O_3-Y_2O_3 and Al_2O_3-Yb_2O_3 systems respectively. The authors attributed this behaviour to differences in intergranular chemistry.

Hardness to Structure Relationship

Hardness is a material's ability to withstand penetration by a surface contact. Figure 2.19 shows the critical structural factors that determine the hardness of LPSSiC materials.

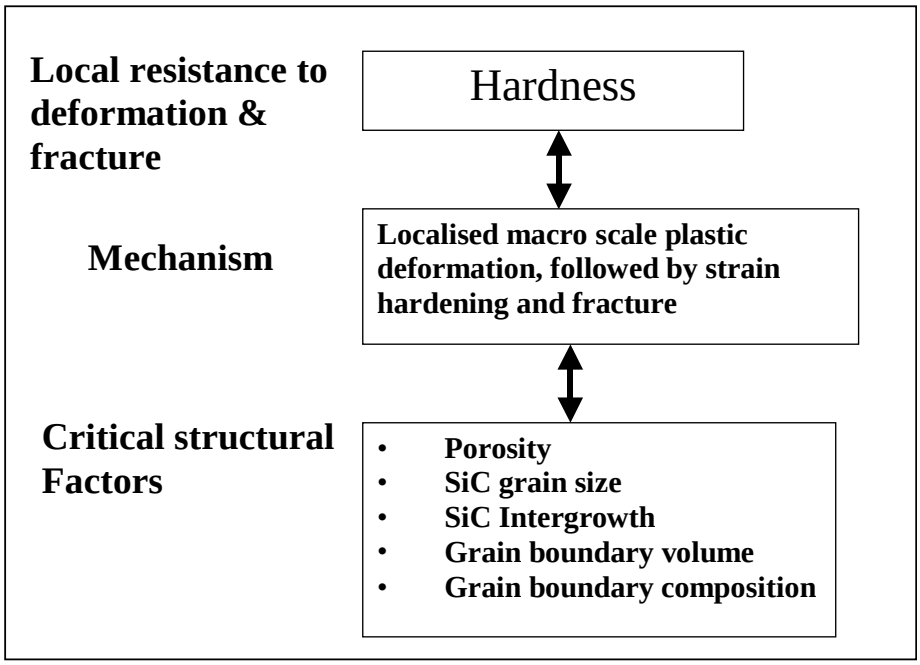


Figure 2.19 Relationship between hardness and critical structural factors for LPSSiC

Baud *et al.*[165] sintered with 3 mass-% YAG additive, and measured grain

sizes in their LPSSiC materials to be between 1.8 and 2.5 μm. The three matrix-seed systems they used produced three different microstructures. The highest hardness values (27 GPa) were observed for the materials with the lowest mean grain diameter (between 0.5 and 1.2 μm). Materials with similar mean grain sizes, but different grain aspect ratios, were also reported to have the same hardness, indicating that the hardness of the materials was mostly determined by the silicon carbide mean grain size. In this work however the grain boundary phase was kept constant (3 mass-% YAG and Al_2O_3).

Baud *et al.*[165] found that hardness was inversely proportional to the square root of the mean silicon carbide grain size, which is similar to what is observed in metals and alloys, where the true hardness is related to mean grain size by equations (2.24) and (2.25)[165], the Hall-Petch relationship:

$$H = 3\sigma_e, \qquad (2.24)$$

where

H= true hardness and σ_e = yield stress.

$$\sigma_e = \sigma_o + k/d^{1/2} \quad \text{(Hall Petch's law)}, \qquad (2.25)$$

where

σ_o = constant same dimensions as stress, k= parameter depending on material, and d= mean grain size.

Vassen *et al.*[112] also observed a decrease in hardness with increase in grain size, in the SSiC materials which they processed. They observed a decrease in hardness from 27 GPa in the material with silicon carbide mean grain size of 0.125 μm, to 23 GPa, in the material with a silicon carbide mean grain size of 0.3 μm.

When Sciti *et al.*[107], hot pressed SiC with 10 mass-% additives, they observed an increase in hardness from 22 GPa in the hot pressed materials to 24.5- 25 GPa after heat treatment, contrary to what was observed by Baud *et al.*[165] and Vassen *et al.*[112]. They attributed it to be due to the reduction of the amount of grain boundary phase due to decomposition reactions that take place during the heat treatments. These decomposition reactions resulted in high mass losses ranging from 3 to 5.5 mass-% in their materials.

She *et al.*[167] observed that the hardness steadily decreased with increase in YAG content, from between 17.3 GPa and 20.1 GPa with 5 mass-% YAG and between 15.6 GPa and 16.8 GPa for 25 mass-% YAG present. The authors explained that this was because of the additive having a lower hardness than silicon carbide. (Note though that no error bars were given in the paper). Samanta *et al.*[114] observed the opposite trend to She *et al.*[167]. They observed an increase in microhardness from 10.7 to 15.5 GPa when YAG content was increased from 10 to 30 mass-% YAG. This was related to an increase in densification with increase in YAG content.

In the case of sintering with Y_2O_3-AlN[118] and Y_2O_3-γ-AlON[117], in which the AlN and AlON form solid solutions with SiC, solid solution hardening is suggested to occur, which is experimentally observed by a maximum in hardness when the AlN and AlON content in the material is increased. This increase in hardness with increase in grain boundary content is contrary to what is generally observed when sintering with the Y_2O_3-Al_2O_3 additive system. When sintering with the AlON system in N_2 the hardness increased from 18GPa with 10 mass-% additive to 28 GPa with 40 mass-% additive[117]. They observed an increase in hardness from 16 to 30 GPa when sintering with 10 mass-% and 50 mass-% AlON additives respectively, sintering in argon. After these maxima in hardness, the hardness decreased again to 26 GPa and 28 GPa at 55 mass-% for the systems sintered in N_2 and Ar respectively. When sintering with AlN

Mandal *et al.*[118] found that hardness increased from 21.2 GPa with 5 mass-% AlN to 25.4 GPa with 25 mass-% AlN.

As described in the "Microstructure to fracture toughness" discussion above, Balog *et al.*[179] did various experiments with β-SiC with Y_2O_3 or Yb_2O_3 or Sm_2O_3 and AlN as sintering additives. They also added either α or β- SiC seeds to the different materials. They found that by adding α-seeds they encouraged the β to α–SiC phase transformation and increased the hardness up to 27.5 GPa. They attributed this to be due to the fact that α-SiC has slightly higher hardness (29 GPa) than β-SiC (28GPa), and also due to the fact that the microstructures with α-seeds were finer. Additionally, Balog *et al.*[179] did nanohardness measurements and observed higher hardness for the core (39.3±2.4 GPa in an α- SiC seeded Y_2O_3-Sm_2O_3 containing material) and lower hardness in the rim of SiC grains in this material (27.4 GPa ± 3.2 GPa). This was attributed to increased SiC-AlN solid solution formation in the rim of the SiC grains.

No references were found in which hot hardness (hardness measured at elevated temperatures) of LPSSiC materials was measured.

Electrical properties

Impedance Spectroscopy (IS) is a relatively new method of characterizing many electrical properties of materials and their interfaces with electronically conducting electrodes. This technique may be used to investigate the dynamics of bound and mobile charge in a material in bulk, or specifically interfacial regions of any kind of solid or liquid material (ionic, semi-conducting, mixed electronic-ionic and insulators (dielectrics))[185].

The electrical measurements are usually made with cells which have two identical electrodes applied to the faces of the sample, which is in the form

of a stubby circular cylinder or rectangular parallelepiped. Measurements can be done in vacuum, argon or oxidizing atmosphere. The general approach is to apply electrical stimulus (voltage or current) to the electrodes and observe the response (resulting current or voltage). This is measured over a range of frequencies, usually between 10^{-2} and 10^{6} Hz, and sometimes up to 10^{9} Hz. The many fundamental microscopic processes and associated phases/ regions in the materials can be considered to have resistive and capacitative components occurring throughout the sample when electrically stimulated. These components all contribute to the overall electrical response.

The negative of the imaginary impedance is usually plotted versus the real impedance and the resultant figure is called a Cole-Cole plot[185]. If the peak frequency (defined below) of a phase lies within range of the instrumentation, an arc will be observed in the Cole–Cole plot for that phase. dc measurements measure the overall resistivity of the material, whereas these ac measurements allow one the possibility of discerning the effects of the different phases in the material. For example when two arcs are observed in a Cole-Cole plot, this means that the electrical properties of two phases is being observed.

The width of the arc in the Cole-Cole plot, which can be read off the base of the arcs on the real impedance axis, is the dc resistance of that phase. This is illustrated in Chapter 3, Figure 3.12.

The dielectric constant is a measure of the charge carriers' response to change in electric field. Because of this high dielectric constants are associated with high conductivity materials with low capacitance[185].

The characteristic frequency of a phase is defined as the frequency observed at the maximum of a Cole-Cole arc, at which the material

changes from primarily conduction to primarily dielectric behaviour. The following equation (2.26) defines the peak frequency:

$$\omega_c = \frac{\sigma}{\varepsilon_o \varepsilon_r} \quad , \qquad (2.26)$$

where,

σ is the conductivity,

ω_c is the peak/ characteristic frequency of the phase, and

$\varepsilon_o\varepsilon_r$ is the relative permittivity of the phase.

Broadbent and Hammersley (1957)[186] introduced the concept of "Percolation Theory", in the form of lattice models, modelling flow of fluid through a static random medium. They discovered that the fluid would not flow unless a certain non-zero number of active bonds or "fluid-carrying channels" was exceeded. This number became known as the percolation threshold (Kirkpatrick 1973)[187]. This theory is a standard model for disordered systems and Shante and Kirkpatrick (1971)[188] suggested that this theory may be able to explain conductor-semiconductor transitions in some disordered solid state systems[189].

In classical percolation theory, it is usually observed that the material has a constant conductivity at low frequencies and an increasing conductivity at higher frequencies, and the increase becomes linear if the measurements are made at high enough frequencies[189].

During liquid phase sintering and subsequent heat treatment there is diffusion of Al outwards from the grain boundary phase and it is thought that Al can substitute Si in the SiC lattice. Different degrees of substitution of Al in the SiC lattice results in the stabilization of different polytypes[4]. Thus the substitution of Al in the lattice influences the ratio of the different polytypes present, which will influence the electrical conductivity of the grain phase. The Al present in the SiC lattice also acts as an electron donor. This means that the grain boundary phase composition (the Al

content in particular) should influence the electrical properties of the material.

The electrical conduction in solids is determined by the charge carrier concentration and mobility. These charge carriers can be electronic or ionic, or a mixture of both. The charge carrier concentration and mobility both contribute to the temperature dependence of electrical conduction. For materials which have a band gap, for example semiconductors such as silicon carbide, both of these processes are temperature-dependent, but the carrier excitation dominates. This results in an Arrhenius type temperature dependence of the conductivity, shown in equation 2.27[190].

$$\sigma \approx \exp\left(-\left(\frac{T_0}{T}\right)^{\gamma}\right), \qquad (2.27)$$

where,

T_0 is associated with the highest phonon energy of the system,

and γ depends on the charge transport mechanism, where it is:

¼ for 3-D variable range hopping, ½ for variable range hopping with Coulombic interactions[191-196] and

1 for activated conduction over a gap (such as semiconductors) and 1D VRH[197].

An alternative representation of the temperature dependence of the conductivity is given by Wang *et al.*[198] in equation 2.28:

$$\sigma = CT^{\eta} \exp\left(-\frac{E_a}{T}\right), \qquad (2.28)$$

where,

C is a constant, E_a is the activation energy for conduction and η depends on the type of mechanism of conduction.

η = 0 for pure non-polar semiconductors,

η = +1 for a highly ionic solid where the large polaron mechanism dominates, and
η = -1 or -3/2 for a polar ionic solid where small polaron mechanism (hopping conduction)[198] operates.

As well-documented in the literature, silicon carbide is a semiconductor. However, the number of groups, which have studied the electrical properties of liquid-phase sintered silicon carbide is limited. Kleebe *et al.*[199], Pesl *et al.*[200] and Siegelin *et al.*[201] did electrical measurements on dense LPSSiC materials sintered with AlN and YAG additives. Volz *et al.*[16,17,18], Martin *et al.*[19,20] and Makrlik *et al.*[21] did electrical measurements on LPSSiC materials sintered with the Y_2O_3-Al_2O_3 sintering additive system. Results showed that materials containing AlN had a higher electrical resistance.

The resistance of the materials was influenced by the secondary phases, consisting mainly of YAG, which made non-Ohmic contacts between the SiC grains[21,201].The specific electrical resistance was found to be dependent on temperature and composition and could span a wide range of values between 10^1 and 10^{12} ohmcm[19, 200,201]. From their results, Siegelin[201] and Pesl[200], developed a model for electrical conductivity through LPSSiC materials. In their model they applied the Brick layer model with conductivity through the SiC grains, and across the grain boundaries. They observed a core-rim structure in the SiC grains and claimed that conductivity through the SiC was influenced by the doping in the rim of the grain.

Martin *et al.*[19,20] proposed electrical conductivity purely along Al-doped rim of the SiC grains. In particular, the SiC-SiC grain contacts were characterized by a concentration of Al-doping. The grain boundaries between these SiC-SiC grains were found to be very narrow. As Martin *et al.* showed with TEM investigations – in some places the grain boundary

thickness was only 2 nm thick. For this reason (because this grain boundary layer was so narrow) they stated that no measurable resistance was observed for the grain boundary.

Kleebe[199], Makrlik[21] and Siegelin[201] made similar observations in their Impedance Specroscopy measurements. They concluded that the resistance was mainly influenced by the edges of the SiC grains and concluded that the resistance of the LPSSiC material can be considered to be made up of a series of low and high resistance components. From these conclusions, Siegelin proposed that the resistance of LPSSIC materials can be calculated by equation 2.29. In this equation the resistance and thickness of the component phases influence the overall resistance. Siegelen[201] proposed that because of the Core-Rim structure, resistance of the SiC component is determined by the resistance of the Core and resistance of the Rim part of the grains.

$$\frac{R}{L} = \frac{1}{d_g} R_g + \frac{1}{d_{gb}} R_{gb}\,, \qquad (2.29)$$

where,
R is the bulk resistance of the material,
R_g and R_{gb} denote the resistance of the grain and grain boundary components respectively, and
d_g and d_{gb} denote the thicknesses of the grain and grain boundary layers respectively.

In general, it was shown that the specific electrical resistance decreased when the sintering/ heat treatment time increased[19,21,201]. This was attributed to the higher SiC grain size observed in the materials sintered for longer times. They concluded that conductivity through the larger more conducting Al-doped rim of the SiC grains decreased the overall resistivity,

accompanied by a reduced influence of the more resistant grain boundary material.

Volz[16,18] also proposed a contribution of the SiC core with carbon impurities in it (from the starting powder), and the formation of an Al-doped rim part of the SiC grains, the result of the solution-reprecipitation during sintering. He acknowledged the contribution of the intergranular grain boundary films on the bulk conductivity in applying the Brick-layer model. However, he did not observe a complete Cole-Cole arc after sintering at 1850^{o}C, and claimed that the Cole-Cole arcs of lower resistances that he observed after sintering at higher temperatures were due to the solution-reprecipitation of silicon carbide. i.e. Al-doping of the rim part of the SiC grains.

LPSSiC materials have a voltage-dependent resistance. Depending on the silicon carbide and grain boundary phase content, the specific resistance can vary: 10^{10} ohmcm measured at room temperature can be reduced by 3 powers of ten (to 10^{7} ohmcm) with increase in applied voltage. This non-Ohmic behaviour was related by Pesl[200] and Siegelin[201] to an energy barrier in the region of the grain boundary. Their assumptions stemmed from models of Halushka[202] and Kondo[203]. The energy barrier in the model could be overcome by means of two possible mechanisms:
One possibility is tunnelling and hopping between localized energy states. The other is thermal activation of electrons to overcome the energy barrier.

In the paper by Volz *et al.*[16], two systems were pressureless sintered and tested. In the first system, SiC powder was synthesized by reaction between Si and C, and this powder was pressureless sintered with small amounts of B and VSi_2. The second system consisted of commercial silicon carbide (H.C. Starck UF25) sintered with 10 vol.-% $3Y_2O_3$:$5Al_2O_3$ molar ratio. Both these systems were sintered in different powder beds.

The powder bed always consisted of SiC at the bottom and Al_2O_3 at the top.

These two systems were pressureless sintered with 1 mass-% VSi_2. and without the VSi_2 in the packing bed, at four different temperatures: 1800, 1850, 1900 and 1950^oC. The specific resistivity of these different materials was measured at room temperature. In general, the lowest sintering temperature resulted in the highest specific resistivity. In the case of the boron and vanadium doped-synthesised SiC powder, the presence of the VSi_2 in the powder bed did not make a significant difference in the specific resistivity of the material. On the other hand, with the sintering of the UF25SiC starting powder with Y_2O_3 and Al_2O_3 sintering additives, the presence of the VSi_2 in the packing bed, significantly increased specific resistivity of the material, especially for the lowest sintering temperature (1800^oC). The resistivities of these resistive materials was increased from the commercial powder to 2 X 10^{10}ohmcm, with the vanadium and boron doping. The authors[16] did not discuss any possible conduction mechanisms.

In other work by Volz *et al.*[17], one composition of the Y_2O_3-Al_2O_3 sintering system, $3Y_2O_3$:$5Al_2O_3$ molar ratio, was pressureless sintered in a powder bed of SiC and Al_2O_3. Sintering was done between 1500 and 2000^oC, for 30 minutes, under an argon atmosphere. Ac (impedance spectroscopy) and dc electrical measurements were done on these materials. Volz *et al.*[17] made the following conclusions:

1) For the materials sintered at 1950^oC, grain boundary resistivity was independent of the amount of secondary phase.
2) For sintering between 1850 and 1950^oC the secondary phase had no influence on the bulk resistivity.
3) Increasing sintering temperature resulted in a decrease in SiC grain resistivity.

4) dc resistivity of LPSSiC depended on the sintering mechanism, specifically that the solution-reprecipitation mechanism (in LPS) decreases resistivity.

In this work[17] no possible conduction mechanisms were discussed. In the impedance spectroscopy measurements of Martin *et al.*[19,20] and Volz *et al.*[16,17,18], they assumed that the arc observed in their Cole-Cole plots was due to silicon carbide. They suggested that doping of silicon carbide dominated the conductivity behaviour of the LPSSiC materials. A shortcoming in both these authors' work, was that they did no temperature-dependence measurements of the electrical properties of the phases observed in the Cole-Cole plots.

Schroeder *et al.*[190] did temperature measurements on solid-state sintered silicon carbide materials, in which boron doping has an influence on the conductivity of the materials. In this study, variable range hopping was observed as the conduction mechanism below 220K, whereas Arrhenius semiconductor behaviour was observed above 220K. Activation energies above 220K were found to be between 257 meV and 262meV were observed, which are comparable to the activation energy determined for boron-doped SiC single crystals[204].

In summary: the papers in literature claim that the electrical properties of silicon carbide ceramics in general, and for the LPSSiC materials in particular, strongly depended on the type and amount of doping. The grain size, the grain boundary, as well as the grain boundary phases, influenced the electrical properties of the materials. However, none of the papers found on electrical measurements of LPSSiC materials (with the Y_2O_3-Al_2O_3 system in particular) determined the temperature dependence of the phases observed in the Cole-Cole arcs.

2.6.6 Material applications

Abrasive wear volume has been shown to decrease as hardness of a material increases. High hardness (in fine ceramics) in turn results in increase in wear resistance of the ceramic[205]. Therefore, a material like silicon carbide, which is an intrinsically hard material (9 on the Mohs scale of hardness), combined with a fine microstructure, produces a material of high wear resistance. With these properties silicon carbide materials are most commonly used as abrasives.

Silicon carbide is also used in heating elements. Better microstructural control of LPSSiC materials, would allow for better control of electrical resistivity of such materials. This would be very useful in the making of LPSSiC heating elements.

LPSSiC materials are used as dewatering elements in the paper machinery and as rings for highly stressed gas seals. These materials have the advantage of being cheaper than silicon nitride materials, and have higher hardness and wear resistance than alumina and tungsten carbide. An additional special application of LPSSiC is as a neutral matrix, in ceramic matrix composites containing plutonium in thermal or fast reactors[206].

Liquid phase sintered silicon carbide can be economically viable for the production of low-temperature wear parts and for heat engine components such as valves, valve seats, piston pins, seals etc.[40].

2.7 Motivation for the research objectives and structure of experimental work

The objective of this project was to investigate relationships between

microstructure formation and mechanical and electrical properties of liquid phase sintered silicon carbide (LPSSiC) materials, which were sintered using different densification techniques (hot pressing, gas pressure sintering, and ultra-high pressure sintering).

2.7.1 Motivation for research project

Little has been published on the fundamental properties of LPSSiC materials. Also, since the field of research in LPSSiC materials is still relatively young (about 10 years old), very little understanding about the relationship between different microstructures, especially grain boundary phases in the Y_2O_3-Al_2O_3 system, and fundamental properties of LPSSiC has been uncovered. In particular, there is a lack of research in the field of electrical studies of LPSSiC systems and ultra-high pressure sintering with LPSSiC systems. This has been illustrated in the above sections regarding the relationship between the grain boundary phases and the mechanical and electrical properties of LPSSiC materials. Silicon carbide is a widely used technical ceramic. It's high hardness, together with the advantages of liquid phase sintering and post-sintering heat treatment, which increases the fracture toughness and strength of this material, give it a wide range of applications and makes this a worthwhile study to pursue.

Successful completion of this study, would enhance our understanding of the useful properties of the material; this in turn will give the chance for better control of the processing, contributing to an improved ability to produce silicon carbide-based materials with the properties for particular applications.

To achieve the objectives of this study, the experiments, described in the following section, were planned.

2.7.2 Structure of experimental work

Liquid phase sintered silicon carbide ceramics were sintered using different densification techniques, namely hot pressing, gas pressure sintering and ultra-high pressure sintering. The hot pressed and gas pressure sintered samples were sintered at 1925^{o}C and post-sinter heat-treated at 1925^{o}C for 1.5, 5 and 8 hours; sections of samples also underwent post-sintering heat treatment at 1975^{o}C for 5 hours. Densification kinetics during hot pressing was measured. After sintering, the materials were systematically analysed to determine relationships between microstructure/phase evolution during heat treatment and mechanical and electrical properties.

The main set of materials, were sintered with 10 mass-% sintering additives, which consisted of a mixture of ytttria and alumina. Based on the yttria-alumina binary phase diagram in Figure 2.20, four compositions (with different yttria: alumina mol ratios) were selected and mixed with the silicon carbide. The one composition in Figure 2.20 in brackets was hot pressed and gas pressure sintered, but not heat treated. After mixing, the powders were processed in different ways depending on the densification technique to be used.

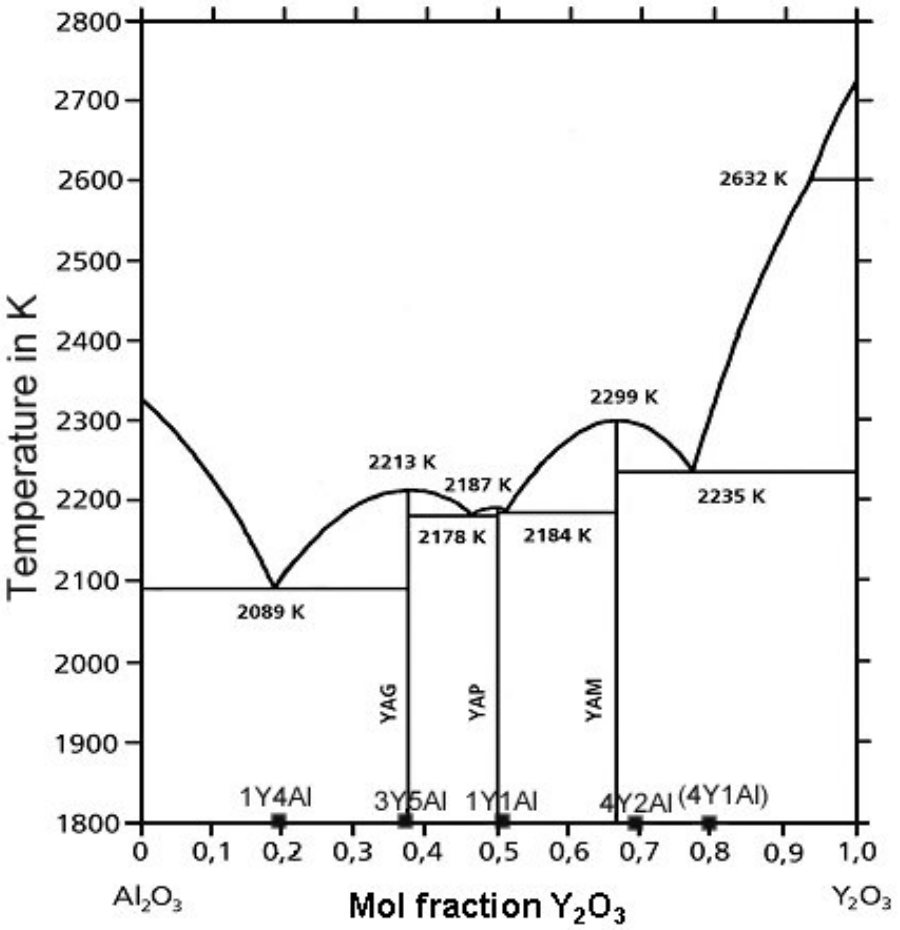


Figure 2.20 Al_2O_3- Y_2O_3 binary phase diagram

To obtain LPSSiC materials with various structures and chemistries, the following set of variables was selected:

(i) yttria: alumina mol ratio

(ii) sintering additive content

(iii) densification technique

(iv) post-sintering heat- treatment time

The objective of the ultra-high pressure sintering in this work was to examine the effect of the ultra-high pressure sintering on the microstructural development of the different compositions LPSSiC materials, which had already been studied during hot pressing and gas

pressure sintering. For this reason α-SiC was used in ultra-high pressure sintering, as in the hot pressing and gas pressure sintering experiments, and not β-SiC.

Work in the literature[13] showed that effects of grain growth and improving fracture toughness depended on post sintering heat treatment at high temperature. For instance, Kim *et al.*[13] found improved fracture toughness for certain materials with 4 hours heat treatment at 1950^{o}C. Therefore it was decided to do heat treatments for 1.5 hours, 5 hours and then heat-treatment for 8 hours to determine relationships between the different microstructures and fracture toughness.

These variables were selected with the objective to obtain discernable structural and grain boundary chemistry differences, which would result in establishing a cause and effect relationship between structure and properties. The processing variables were expected to produce materials with varying amounts of YAG phase in the grain boundary material, together with other grain boundary phases, and also possibly materials with different SiC polytype ratios (because of the expected stabilisation of different polytypes by Al doping in the SiC lattice during heat treatment). The differences in grain boundary composition were expected to affect the grain growth and other material changes during post-sintering heat treatment.

To achieve the objectives of a project which involves microstructure-properties relationship determination, one needs tools to quantify not only the properties, but also the microstructure, in order to produce more objective results. The microstructure of a material can be classified according to the phase composition, as well as the distribution of the phases.

To determine extent of densification, the Archmides density of the samples

was measured. Impurity content was measured using the X-Ray Fluorescence (XRF) technique. The accurate quantitative phase analysis of silicon carbide-based ceramics is not easy because of the significant overlap of the Bragg reflections from the different SiC polytypes. The Rietveld refinement method is a powerful tool for the accurate and precise analysis of the phase/polytype compositions in these materials. A computer program (Autoquan) provided the "Rietveld code" for the necessary accurate quantitative phase determination. To quantify grain size distribution, an "IMAGANALYSIS"- based program was used for the quantitative analysis of the FESEM images of all the samples produced and heat treated in the research project.

The mechanical properties which were studied in this work are Vicker's hardness, indentation toughness, four point bending strength and elastic modulus. The cracks resulting from the indentation tests were studied using a SEM. The study of crack propagation in LPS materials has been done quite extensively in silicon nitride based ceramics[174,175], but not in silicon carbide ceramics. There are three main approaches to studying crack paths: measuring the roughness of the crack path (which is related to how much intergranular fracture there is in the material, as opposed to transgranular fracture); measuring the amount of crack bridging, and measuring the ratio of intergranular to transgranular fracture[10,11]. The objective of the crack studies was to predict which toughening mechanism was dominant in which material, i.e. in which materials crack bridging dominated.

To study electrical behaviour of liquid phase sintered silicon carbide, impedance spectroscopy is a useful tool that was used, since this method allows one to obtain information about the electrical conductivity of the bulk of the material, as well as of individual phases in the material. The temperature dependence of the phases in the material, can also give one information about the conduction mechanism.

The general plan for the project is outlined in Figure 2.21.

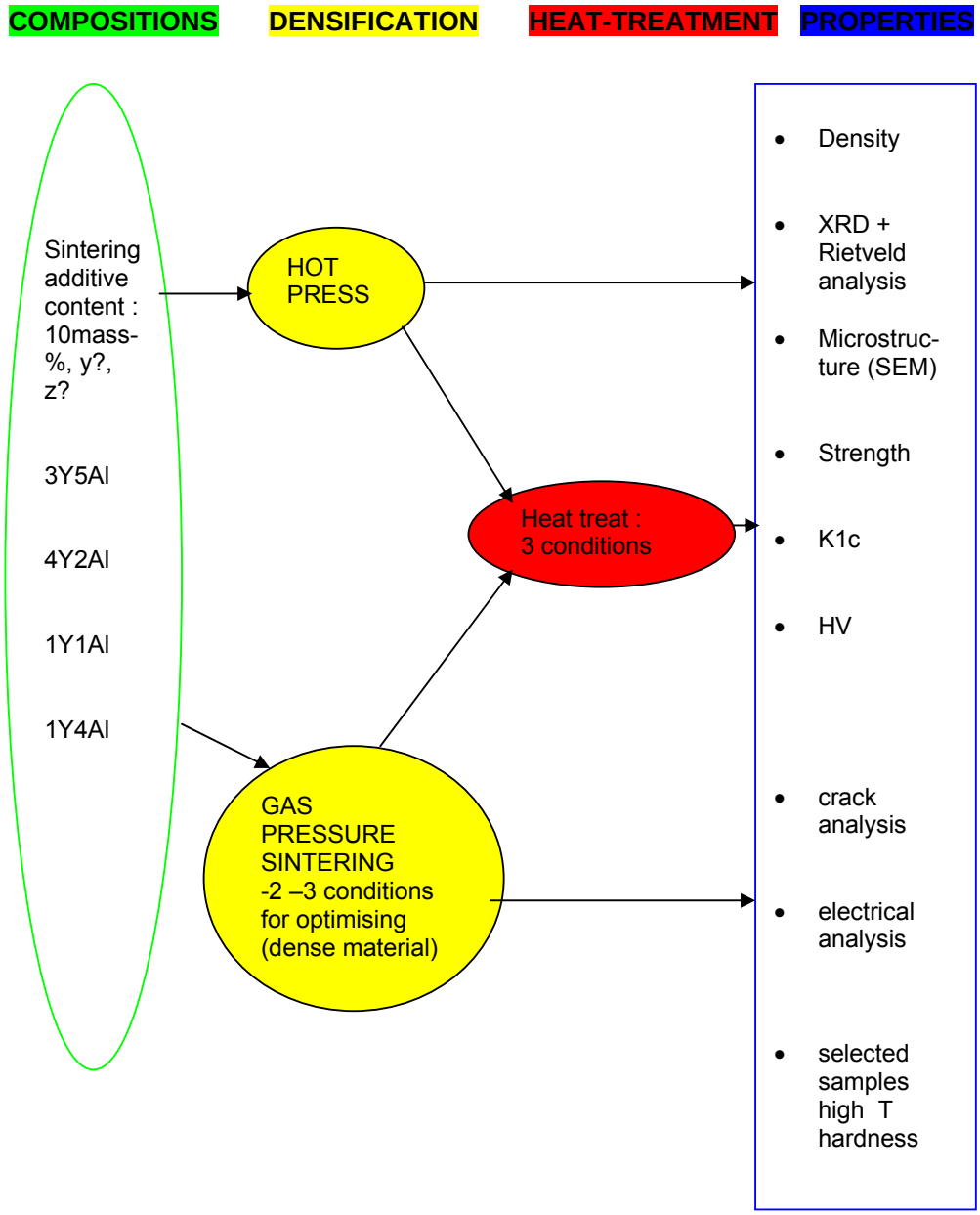


Figure 2.21 Flow chart of experimental plan

Note that y = 4 - 5 mass%, z = 15 mass%

y and/or z employed if difference between heat treated samples, different compositions, is not significant enough .

Y = Y_2O_3, Al = Al_2O_3.